

EnduroSharp™ Nonmetallic (Torlon®) Aircraft Maintenance Tools

Paul K. Childers^{1,2}, Brett A. Bolan¹, and James J. Mazza¹

Air Force Research Laboratory,

¹Materials and Manufacturing Directorate

2179 12th Street

Wright-Patterson Air Force Base, OH 45433-7718

²University of Dayton Research Institute

300 College Park

Dayton, OH 45469-0051

ABSTRACT

The lack of reliable and effective nonmetallic material removal tools available to maintainers drives the continued use of unapproved tools and/or methods when removing materials from aerospace vehicles. The use of metallic tools has resulted in damage to vehicles, both short term and long term, causing the need for expensive repairs and reduction in vehicle availability.

The University of Dayton Research Institute under contract to the Air Force Research Laboratory has developed and commercialized a series of nonmetallic material removal tools under the “EnduroSharp” trademark manufactured from glass-filled Torlon thermoplastic produced by Solvay Engineered Plastics. The use of this material coupled with the tools’ designs is responsible for their superior stiffness and durability (resistance to chemicals and heat) and enhance the tools’ ability to maintain sharp cutting edges, allowing efficient removal of coatings, boots, tapes, sealants, gap fillers and caulking materials, pressure sensitive adhesive (PSA), and tape residue without damaging underlying composite surfaces.

Copyright C: This paper is declared a work of the U.S. Government and is not subject to copyright protection.

1. INTRODUCTION

1.1 Background

The lack of reliable and effective nonmetallic material removal tools available to maintainers drives the continued use of unapproved tools and/or methods when removing materials from aerospace vehicles. The use of metallic tools has resulted in damage to vehicles, both short term and long term, causing the need for expensive repairs and reduction in vehicle availability.

In an effort to eliminate damage and adverse effects on aircraft availability attributed to the use of unauthorized material removal tools and processes, the Air Force Research Laboratory (AFRL) and the University of Dayton Research Institute (UDRI) developed a series of nonmetallic material removal tools fabricated from Solvay Engineered Plastics Torlon thermoplastic. The state-of-the-art Torlon polyamide-imide (PAI) has excellent toughness, high strength, and high stiffness at temperatures up to 260°C (500°F). Additionally, this material's broad chemical resistance extends to strong acids, solvents and aerospace fluids, allowing the tools to be used as part of authorized heat or chemical-assisted removal processes to expedite material removal. Unlike traditional polymers, the thermoset-like properties of these tools enable the blades to withstand the high heat and friction of machining and sharpening, allowing repeated use.

The tools' designs and material combinations enhance their durability and ability to maintain a sharp cutting edge, providing a more efficient, safer method of removing coatings, boots, tapes, sealants, gap fillers and caulking materials, as well as pressure sensitive adhesive and tape residue, without damaging underlying composite structure.

The approach adopted to develop enhanced nonmetallic material removal tools began with identifying the areas on aerospace vehicles requiring material removal and the types of materials that must be removed. In addition, ineffective nonmetallic material removal tools currently used were identified (Figure 1) and their deficiencies were studied to understand improvements required for new tools.



Figure 1. Ineffective Nonmetallic Material Removal Tools

Furthermore, unauthorized metallic tools and methods (Figure 2) were also evaluated to determine the attributes that allow them to effectively remove identified materials.



Figure 2. Typical Unauthorized Tools and Methods

This paper addresses three tool geometries/types that were identified for development: the Gap Filler Removal Bit (GFR-Bit), the Torlon Scraper Blade (TSB), and the Torlon Gap Blade (TGB), as shown in Figure 3.

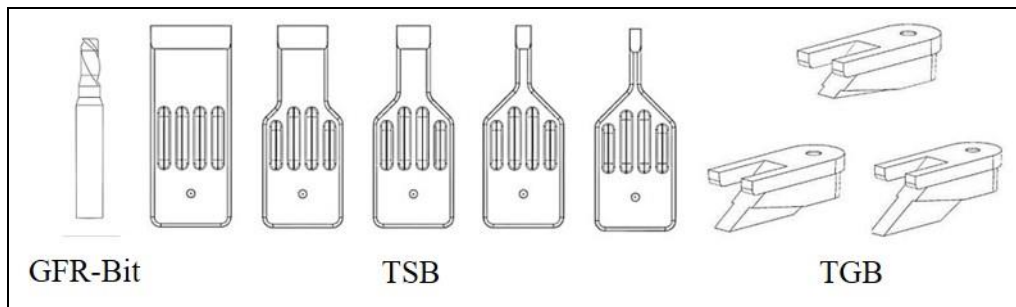


Figure 3. Nonmetallic Tool Geometries/Types

Knowledge regarding the relevant removal applications and lessons learned from use of the existing tools were key to not only developing improved removal tools but also demonstrating better techniques for applying the tools.

2. GAP FILLER REMOVAL BIT (GFR-BIT)

The first improved material removal tool developed was the rotary GFR-Bit. Significant work was focused on material selection for this tool, leading to the selection of glass-filled Torlon thermoplastic used for all of the new removal tools developed by UDRI and AFRL.

2.1 Prototype Development

The GFR-Bit was developed to remove certain materials from a gap of specific dimensions, approximately 6 mm wide by 6 mm deep (0.25 in x 0.25 in). Tools required to drive the bits, such as pneumatic and cordless drills and die grinders, also had to be selected, and their capabilities and operating procedures were dependent on the GFR-Bit material and configuration. Metallic rotary bits that could remove the relevant materials at desirable rates from the specified gap were identified to guide GFR-Bit development (Figure 4).

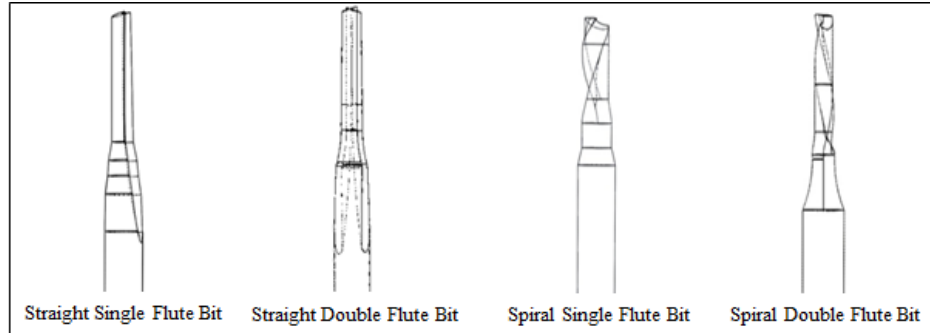


Figure 4. Selected Metallic Bit Configurations

Once GFR-Bit configurations were identified for evaluation, a prototype mold was fabricated of the metallic bit using modeling clay and a Mold Max[®] series silicone rubber from Smooth-On, Inc. The GRF-bits were cast by pouring Smooth-On TASK[®] 8 heat-resistant polyurethane resin into the silicone rubber mold cavity. The prototype mold and GRF-bits are shown in Figure 5.



Figure 5. Prototype Mold and Bits

For this evaluation, both carbon/epoxy and carbon/bismaleimide (BMI) test panels were fabricated. Each measured approximately 30.5 cm long by 30.5 cm wide by 13 mm thick (12.0 in x 12.0 in x 0.5 in). Approximately 6 mm wide by 6 mm deep (0.25 in x 0.25 in) grooves were machined into the test panels at intervals along their entire lengths, and the gaps created were filled with flexibilized epoxy materials (Figure 6).

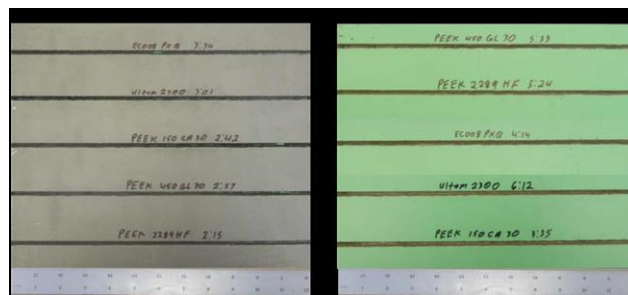


Figure 6. Test Panels

The prototype GRF-bits, mounted in a Dewalt battery-powered electric drill, successfully removed limited amounts of gap filler from the gaps before breaking. Smooth-On TASK 8 polyurethane resin lacked the stiffness and durability required to remove acceptable amounts of flexibilized epoxy gap filler, indicating a more robust material was required.

Unfilled Ultem® 1000 (polyetherimide resin) and Ultem 2300 (30 percent glass fiber reinforced) were selected to fabricate the next versions of GFR-Bits. The Ultem materials are produced in pellet form (Figure 7) and cannot be poured into a mold as was done with the TASK 8 heat-resistant polyurethane resin.



Figure 7. Ultem Pellets

The Ultem materials had to be processed using injection molding equipment (Figure 8) due to the materials' inherently high-temperature melting points and viscosities.



Figure 8. Injection Molding Equipment

This required the design and manufacturing of a low-grade steel prototype injection mold tool (Figure 9) to make a limited run of prototype GRF-bits using the Ultem materials.

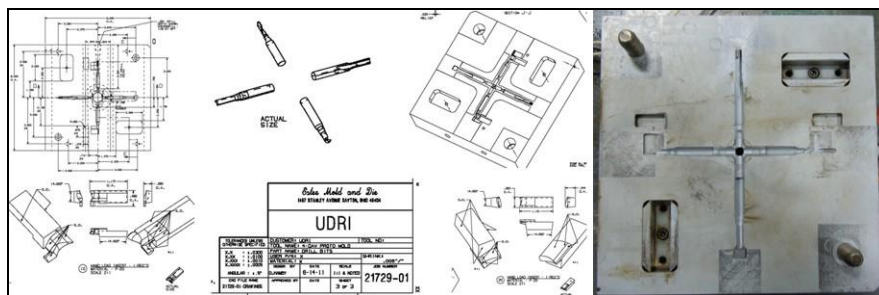


Figure 9. Prototype Injection Mold Design and Mold

Estee Mold and Die (Dayton OH) manufactured a prototype injection mold tool and Priority Custom Molding, Inc. (Dayton OH) produced a limited production run of each configuration GFR-Bit with the two materials. Figure 10 shows the four different configurations of GFR-Bits after removal from the mold and after separation from the spurs.



Figure 10. Ultem 1000 and Ultem 2300 GFR-Bits

2.2 Prototype Demonstration

The GFR-Bits were mounted on a 20,000 revolutions per minute (rpm) Dotco[®] 90-degree grinder (model 12L1281-36), as shown in Figure 11, connected to a 620 kPa (90 psi) compressed air source.



Figure 11. Dotco (20,000 rpm) 90-degree Grinder

Both Ultem 1000 and Ultem 2300 GFR-Bits successfully removed small sections of flexibilized epoxy gap filler from test panel gaps before failing (Figure 12).



Figure 12. Ultem 1000 and 2300 GFR-Bit Demonstration

Although the demonstration was successful in illustrating Ultem GFR-Bits could remove gap filler without damaging the test panels and do so much more efficiently than GFR-Bits manufactured from Smooth-On TASK 8 polyurethane resin, Ultem GFR-Bits still lacked the durability necessary to remove more than about 15 cm (6 in) of material before failing. The target gap filler removal length for this project was over 91 linear centimeters (36 in) to be removed by one bit.

The single flute spiral GFR-Bit was eliminated from future consideration due its lack of durability. These small diameter bits lacked the stiffness required to engage and remove the gap

filler, breaking off where the fluted section meets the shoulder area of the GFR-Bit upon engaging the gap filler.

Input from the Ultem injection molder identified several materials that would provide additional stiffness and durability with the identified configurations, but GFR-Bit fabrication for evaluation required a different injection molding company that specialized in the identified materials.

Additional GFR-Bits were produced using the following materials:

- Polyether ether ketone (PEEKTM):
 - Unfilled (450G)
 - 30 percent carbon fiber reinforced (150CA30)
 - 30 percent glass fiber reinforced (450GL30)
 - 50 percent carbon fiber reinforced (2289 HF)
- Polyether ketone (PEKKTM) + polybenzimidazole (PBI)
- LNPTM ThermocompTM Compound EC008PXQ (Polyetherimide - 40 percent chopped carbon fiber reinforced)
- Ultem 1000 and filled Ultem 2300 (30 percent glass fiber reinforced) for comparison baseline (vendor to vendor)

The GFR-Bits were mounted on the same 20,000 rpm grinder used previously, which was fitted with a inline air regulator, as shown in Figure 13, to enable line pressure adjustment and allow for the evaluation of the effects of varying grinder rpm.



Figure 13. Dotco (20,000 rpm) 90-degree Grinder with Regulator

Each GFR-Bit configuration/material composition was evaluated using the Dotco grinder connected to a 620 kPa (90 psi) compressed air source with the inline regulator set to 69 kPa (10 psi). With the grinder running at full speed, the GFR-Bit under evaluation was located over the gap and plunge driven into the gap filler slowly, allowing the bit to cut through the gap filler until the bottom of the gap was reached. The GFR-Bit was then moved lengthwise through the gap filler using light to moderate hand pressure on the grinder (Figure 14); occasionally the GFR-Bit was partially removed to facilitate debris removal from the gap.

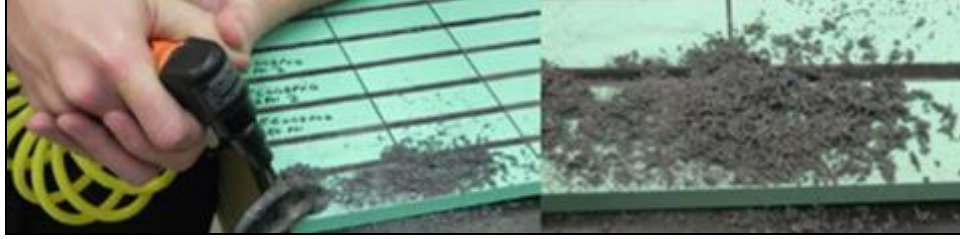


Figure 14. Gap Filler Removal

The evaluation showed all three remaining GFR-Bit configurations under consideration could remove the gap filler. However, using 69 kPa (10 psi) line pressure, the straight single flute and straight double flute GFR-Bits required extreme care when inserting them into a gap. These GFR-Bits would chatter and break (Figure 15) due to their asymmetrical cutting surfaces operating at slow speed.



Figure 15. Typical Failure of Straight Single and Double Flute GFR-Bits

The spiral single flute bit proved to be the most durable of the GFR-Bits for removing gap filler, so this configuration was the only one selected for further evaluation in this program.

2.3 Spiral Bit Prototype Evaluation

Although the spiral single flute bit on a grinder driven by 69 kPa (10 psi) line pressure was the only robust configuration identified during initial tests with GFR-Bits, performance was not ideal since the grinder became sluggish when removing gap filler and operated at inconsistent revolutions per minute as force was applied. Due to the variations in output speed when operating the grinder at 69 kPa (10 psi), an evaluation was performed to determine a better line pressure when using the 20,000 rpm grinder with the selected GFR-Bits. Gap filler was removed from a test panel (Figure 16) using line pressures of 69, 172, and 551 kPa (10, 25, and 80 psi). A line pressure was desired that allowed removal of gap filler using the 90-degree grinder and selected GFR-Bits without bogging down or exceeding the service temperatures of the gap filler or GFR-Bit materials.

With the test panel marked off in 76.2 mm (3 in) test sections (Figure 16), a spiral single flute GFR-Bit was used to remove gap filler from each of the test sections at the different pressure line settings.

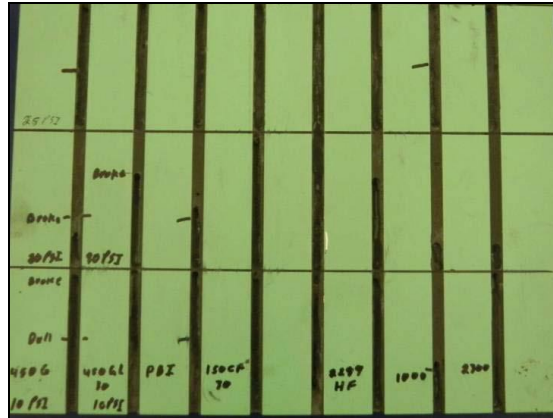


Figure 16. Test Panel

The GFR-Bits were composed of PEKK + PBI, PEEK 150CA30, PEEK 450G, PEEK 450GL30, PEEK 2289 HF, Ultem 1000, and Ultem 2300. Images of the GFR-Bits after gap filler removal at the various line pressures are provided in Figure 17.

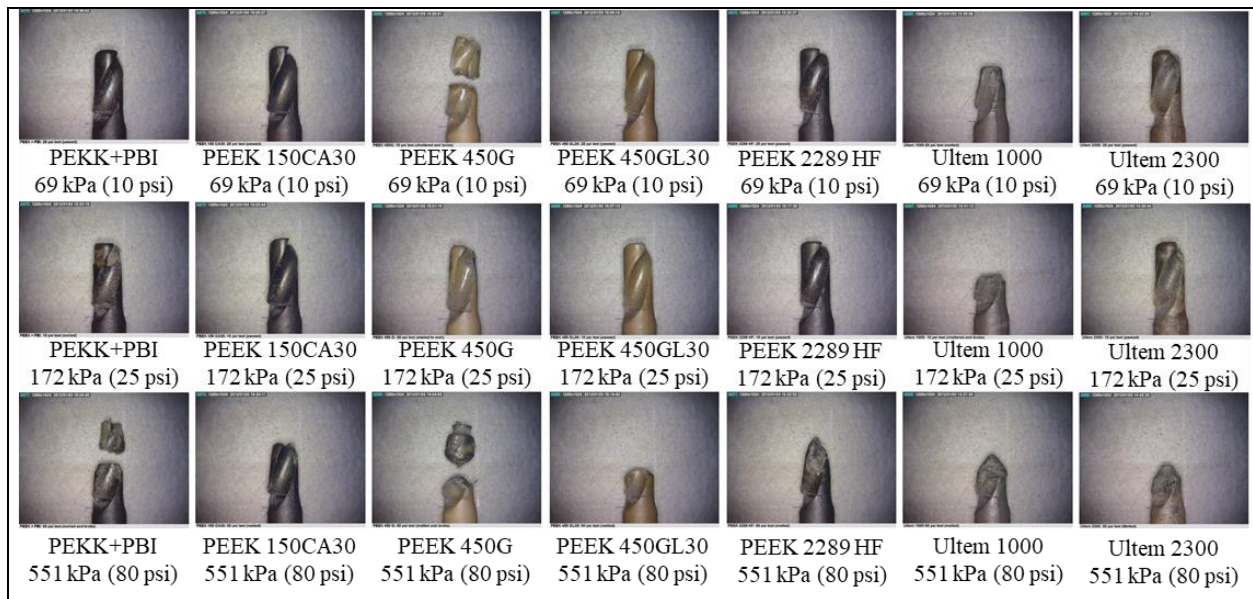


Figure 17. Bit Performance Evaluation Results

Of the three evaluated operating pressures, the most favorable pressure appeared to be 172 kPa (25 psi) for the majority of the GFR-Bit materials. The grinder had a greater propensity of bogging down and running at inconsistent rpm when operated with 69 kPa (10 psi) line pressure. At 551 kPa (80 psi), all of the GFR-Bits began to melt soon after engaging the gap filler, as can be seen in the bottom row images of Figure 17.

Although 172 kPa (25 psi) was identified as the most favorable operating pressure, the three GFR-Bit materials that did not contain fillers exhibited excessive wear and damage (Figure 18). For this reason, PEKK + PBI, PEEK 450G, and Ultem 1000 were removed from further consideration, whereas PEEK 150CA30, PEEK 450GL30, PEEK 2289 HF, and Ultem 2300 materials were selected for further evaluation.

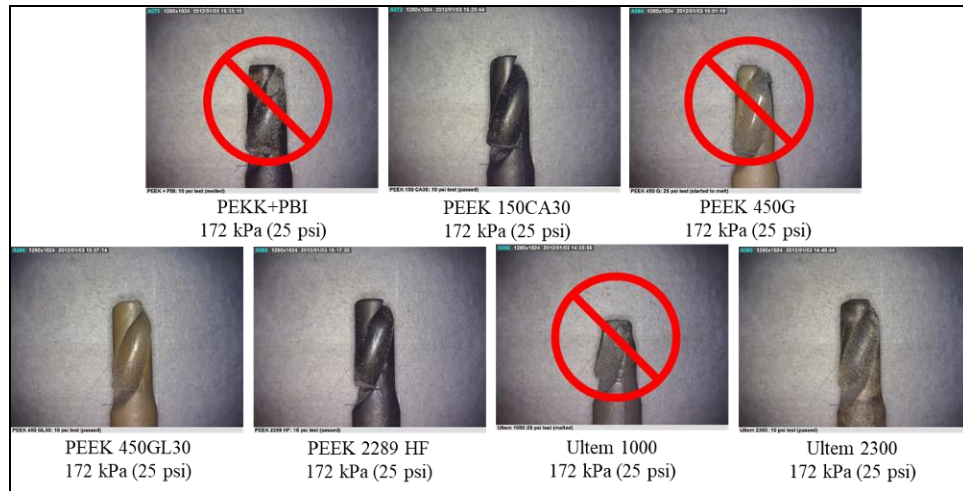


Figure 18. Selection of GFR-Bit Materials

Spiral single flute GFR-Bits manufactured with these selected materials, as well as similar bits fabricated from LNP Thermocomp Compound EC008PXQ, were then used to remove two types of flexibilized epoxy gap filler, identified as “old” and “new,” from a 30.48 cm (12.0 in) gap length. The bits were photographed before and after removal of old gap filler, as shown in Figure 19 and Figure 20, respectively. The mass of each GFR-Bit was obtained before and after gap filler removal to determine mass loss during the removal process.



Figure 19. Pristine GFR-Bits



Figure 20. GFR-Bits after Removing Old Gap Filler

In addition, the time to remove 30.48 cm (12.0 in) of old gap filler was recorded using a stopwatch; Table 1 provides details for the GFR-Bit removal evaluations on old gap filler.

Table 1. Removal Details for Old Gap Filler

Material Group	Bit Material	Material Removed (Old Filler)	Time	Bit Initial Weight (Grams)	Bit Post Weight (Grams)	Material Loss (Grams)	Percent Loss
LNP	EC008PXQ	30.48 cm x 5.08 mm x 4.5 mm (12.0 in x 0.200 in x 0.180 in)	00:04:14	1.4415	1.433	0.0085	0.59
Ultem	2300	30.48 cm x 5.08 mm x 4.5 mm (12.0 in x 0.200 in x 0.180 in)	00:06:12	1.4977	1.4879	0.0098	0.65
Peek	150CA30	30.48 cm x 5.08 mm x 4.5 mm (12.0 in x 0.200 in x 0.180 in)	00:03:35	1.3451	1.3417	0.0034	0.25
	450GL	30.48 cm x 5.08 mm x 4.5 mm (12.0 in x 0.200 in x 0.180 in)	00:05:33	1.4063	1.3967	0.0096	0.68
	2289HF	30.48 cm x 5.08 mm x 4.5 mm (12.0 in x 0.200 in x 0.180 in)	00:05:24	1.4409	1.4325	0.0084	0.58

Images of the GFR-Bits after removing 30.48 cm (12.0 in) of new gap filler are provided in Figure 21.



Figure 21. GFR-Bits after Removing New Gap Filler

Again, the time to remove 30.48 cm (12 in) of the new gap filler was recorded using a stopwatch, with details documented in Table 2.

Table 2. Removal Details for New Gap Filler

Material Group	Bit Material	Material Removed (New Filler)	Time	Bit Initial Weight (Grams)	Bit Post Weight (Grams)	Material Loss (Grams)	Percent Loss
LNP	EC008PXQ	30.48 cm x 6.35 mm x 4.5 mm (12.0 in x 0.250 in x 0.180 in)	00:03:34	1.4414	1.4247	0.0167	1.16
Ultem	2300	30.48 cm x 6.35 mm x 4.5 mm (12.0 in x 0.250 in x 0.180 in)	00:03:01	1.5012	1.4931	0.0081	0.54
Peek	150CA30	30.48 cm x 6.35 mm x 4.5 mm (12.0 in x 0.250 in x 0.180 in)	00:02:42	1.3471	1.3406	0.0065	0.48
	450GL	30.48 cm x 6.35 mm x 4.5 mm (12.0 in x 0.250 in x 0.180 in)	00:02:57	1.4011	1.3976	0.0035	0.25
	2289HF	30.48 cm x 6.35 mm x 4.5 mm (12.0 in x 0.250 in x 0.180 in)	00:02:15	1.4400	1.4283	0.0117	0.81

All five materials used in the timed trials performed well, successfully removing the 30.48 cm (12.0 in) of gap filler with negligible GFR-Bit material loss and with minimal effort on the part of the operator.

After consulting with the injection molder on the results of these trials, a suggestion was made to evaluate Torlon in an attempt to further improve GFR-Bit durability. Three formulations of Torlon, obtained as pellets, were used to manufacture (injection mold) additional GFR-Bits:

- 4301: 12 percent graphite powder and 3 percent Polytetrafluoroethylene (PTFE) filled PAI
- 4275: 20 percent graphite and 3 percent PTFE filled PAI
- 5030: 30 percent glass fiber reinforced PAI, providing the greatest degree of dimensional control.

The three Torlon candidates were evaluated in the same manner as the previous materials. Images of the bits prior to the removal trials are shown in Figure 22.



Figure 22. Pristine Torlon GRF-Bits

Images of the bits after attempting to remove 30.48 cm (12 in) of old and new gap filler are shown in Figure 23 and Figure 24, respectively. Additionally, the times required for each bit to remove the gap filler material are provided in Table 3 and Table 4. Torlon 4301 was not evaluated with old gap filler.



Figure 23. Torlon GFR-Bits after Removing Old Gap Filler

Table 3. Removal Details for Old Gap Filler (Torlon GFR-Bits)

Material Group	Bit Material	Material Removed (Old Filler)	Time	Bit Initial Weight (Grams)	Bit Post Weight (Grams)	Material Loss (Grams)	Percent Loss
Torlon	4275	25.5 cm x 5.08 mm x 4.57 mm (5.0 in x 0.200 in x 0.180 in)	00:01:47	1.5048	1.5019	0.0029	0.19
	5030	25.5 cm x 5.08 mm x 4.57 mm (5.0 in x 0.200 in x 0.180 in)	00:03:13	1.6162	1.6116	0.0046	0.28



Figure 24. Torlon GFR-Bits after Removing New Gap Filler

Table 4. Removal Details for New Gap Filler (Torlon GFR-Bits)

Material Group	Bit Material	Material Removed (New Filler)	Time	Bit Initial Weight (Grams)	Bit Post Weight (Grams)	Material Loss (Grams)	Percent Loss
Torlon	4275	25.5 cm x 6.35 mm x 4.57 mm (12.0 in x 0.250 in x 0.180 in)	00:02:26	1.501	1.4862	0.0148	0.99
	4301	16.5 cm x 6.35 mm x 4.57 mm (6.5 in x .250 in x 0.180 in)	00:00:58	1.4621	1.4568	0.0053	0.36
	5030	25.5 cm x 6.35 mm x 4.57 mm (12.0 in 0.250 in x 0.180 in)	00:01:12	1.6385	1.6128	0.0257	1.57

2.4 Final Article Evaluation

Comparing the evaluation results, the top performer among the various materials was Torlon 5030. This material exhibited very minimal wear during gap filler removal and was able to do so in some of the fastest observed times. However, to be an acceptable gap filler removal tool, the GFR-Bit also had to be able to remove material without causing damage to any composite structure encountered.

As noted previously, the supply compressed air pressure was lowered to reduce the speed of the 20,000 rpm grinder to prevent GFR-Bit damage (exceeding material service temperature); however, this degraded the efficiency of the 20,000 rpm grinder due to lost torque. To see if another tool would perform better (without too much loss of torque), a 12,000 rpm Dotco grinder (model 12L1280-36) with reduced line pressure was evaluated. To establish a line pressure for the 12,000 rpm grinder, the rpm generated with the 20,000 rpm grinder operated at 172 kPa (25 psi) was measured using an Extech model 461920 tachometer (Figure 25).



Figure 25. Extech Tachometer

It was determined the 20,000 rpm grinder operated at 172 kPa (25 psi) rotated between 5,900 and 6,700 rpm free spinning (no load applied). The 12,000 rpm grinder was connected to the same compressed air source and the line pressure was adjusted via an inline air regulator until the free spinning rpm reached a range between 6,000 and 7,000 rpm, which occurred at about 241-310 kPa (35-45 psi). Cursory tests using Torlon 5030 GFR-Bits were repeated to ensure the 12,000 rpm grinder with the air regulator set at 310 kPa (45 psi) produced results similar to those observed during earlier evaluations. Results showed material removal rates increased without the grinder bogging down, and less applied force was required to advance the GFR-Bit through the gap filler, so the 12,000 rpm Dotco with 241-310 kPa (35-45 psi) line pressure was adopted.

To verify the GFR-Bits would not cause damage to composite structure, additional test panels were manufactured of carbon/epoxy and carbon/BMI. In service, components are often primed prior to application of gap filler; however, in this evaluation, the test panels were not primed in order to provide a worst-case scenario by allowing direct contact between the panels' composite materials and Torlon 5030 GFR-Bits during gap filler removal from simulated gaps.

An overall image of the test panel configuration is shown in Figure 26. It was fabricated from twelve short pieces of composite material approximately 19.0 mm x 43.1 mm x 6.35 mm (0.75 in x 1.70 in x 0.25 in) fastened to a single composite material base with approximate dimensions of 33 cm x 43.1 mm x 2.54 mm (13 in x 1.7 in x 0.10 in). The short pieces fastened to the base formed 6.35 mm (0.25 in) tall side walls and were spaced to create simulated gaps with widths of 6.35 mm (0.25 in). After fabrication, the test panel was disassembled, photographed and reassembled. A GFR-Bit was activated in each gap for 60 seconds while being moved back and forth in contact with a side wall and the composite base (simulated gap bottom) to produce "impinged" surfaces. After the impingement runs, the test panel was disassembled and photographed. One of the test panel sides and one-half of the impinged base were then cleaned using cotton swabs moistened with acetone and again photographed.

White arrows in Figure 26 identify the sides of the gap, and the black arrow identifies the gap bottom. The double-ended arrow identifies the direction of GFR-Bit movement.

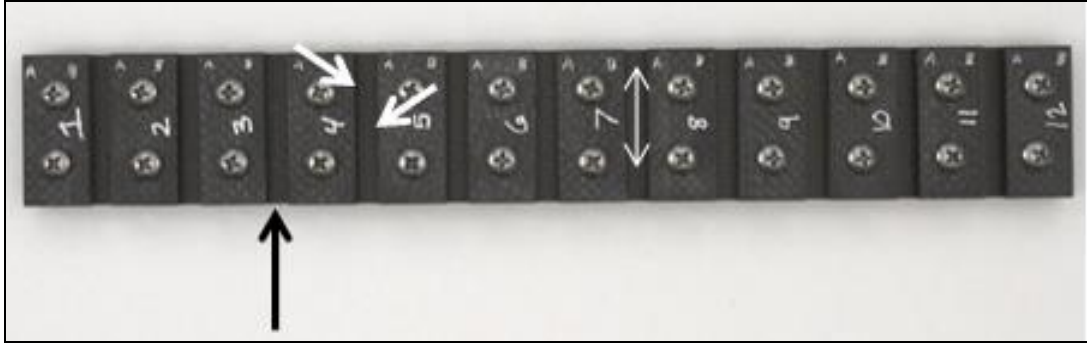


Figure 26. Test Panels Configuration

Figure 27 shows epoxy samples of the baseline (A), uncleaned impinged area (B), and cleaned impinged area (C). The impinged surfaces of the gap side walls revealed transfer of material (fiberglass filler from Torlon 5030).

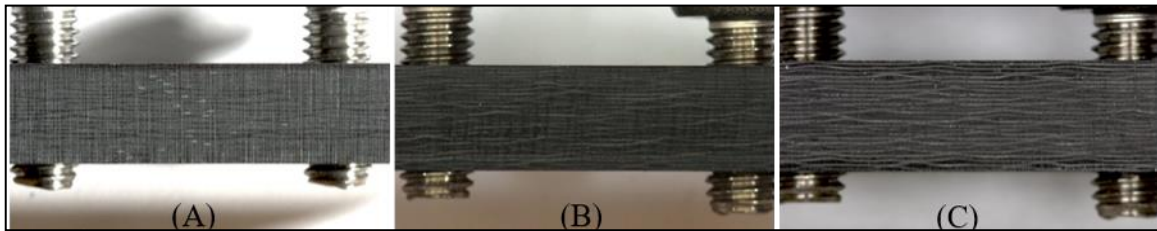


Figure 27. Epoxy Test Panel Gap Side Wall

Images shown in Figure 28 indicate GFR-Bit material transfer to the impinged areas (A and B) of the test panel, as well as remnants of the GFR-Bit material on the impinged area after cleaning (C and D). There were no exposed test panel fiber ends observed (images C and D).

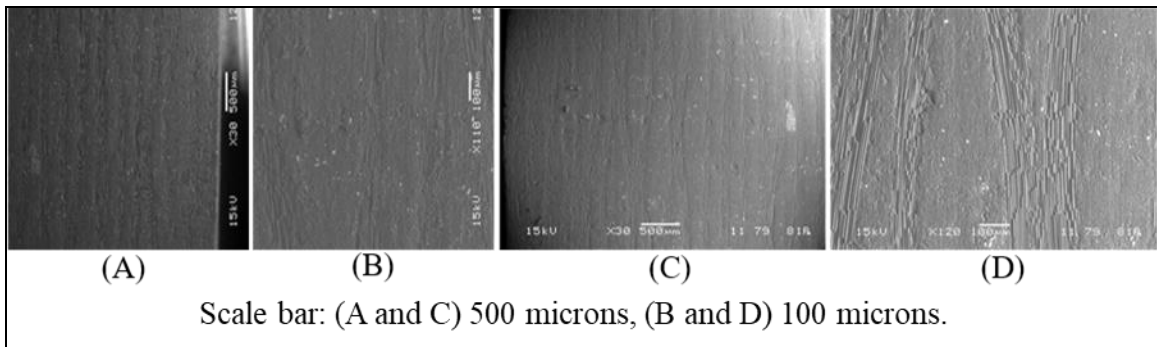


Figure 28. Epoxy Test Panel Gap Side Wall (Magnified)

The epoxy test panel base surface impingement area is shown in Figure 29 before cleaning (A) and after cleaning of one-half of the impinged area, as indicated by the arrow (B).

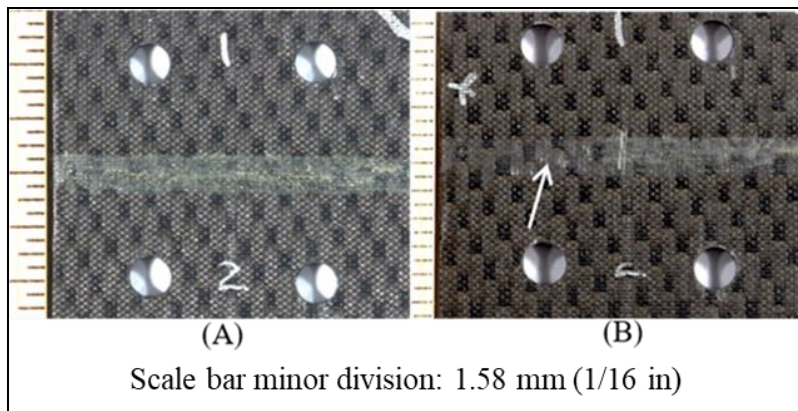


Figure 29. Epoxy Test Panel

Scanning electron microscope (SEM) images in Figure 30 show remnant material (fiberglass and Torlon) transferred to the surface of the test panel base prior to cleaning (A and B) and after cleaning with acetone-moistened cotton swabs (C and D).

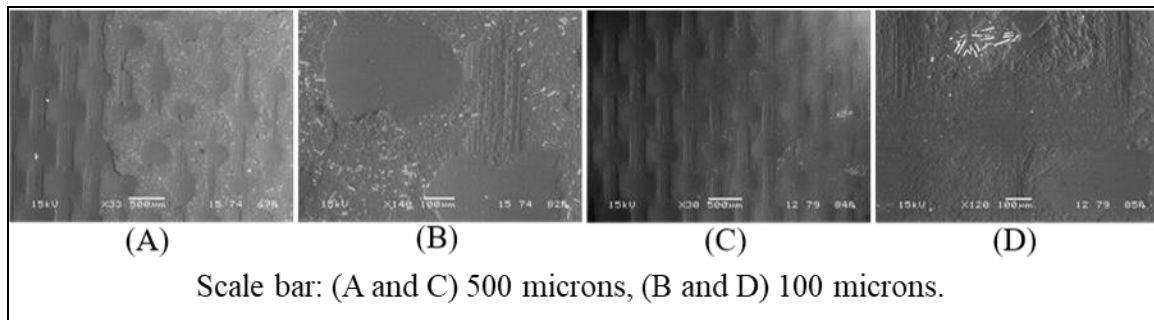


Figure 30. Epoxy Test Panel Base (Magnified)

Images of the impinged GFR-Bit (Figure 31) indicate Torlon material smeared in the area identified by the white arrow (A) and reveal exposed filler fibers, which are shown magnified (C) at the location identified by the black arrow (B).

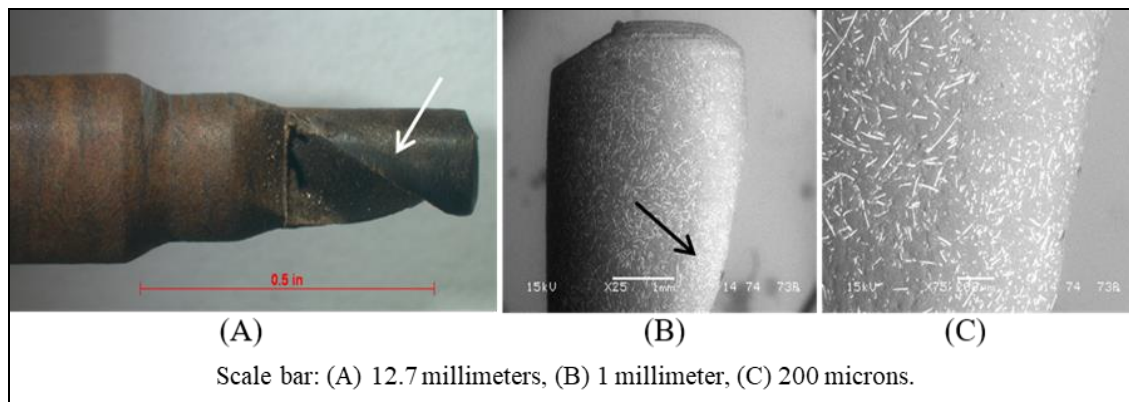


Figure 31. Torlon 5030 GFR-Bit Used on Epoxy Test

Figure 32 shows the baseline (A), uncleaned impinged area (B), and cleaned impinged area (C) BMI samples. The impinged surfaces of the sides evidenced transfer of Torlon 5030 fiberglass filler.

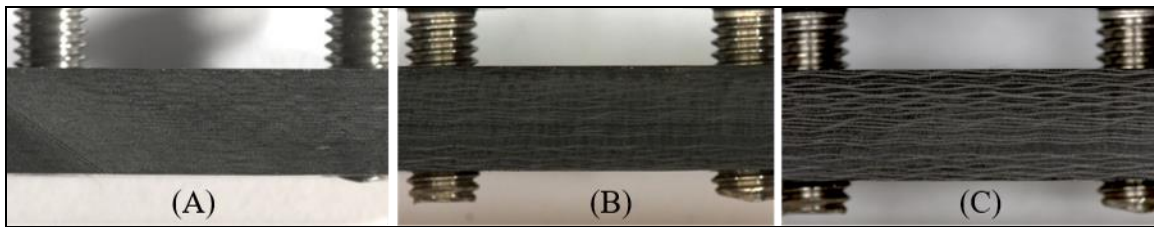


Figure 32. BMI Test Panel Gap Side Wall

Figure 33 provides magnified images of the gap side wall of the BMI test panel after impingement by GFR-Bits before cleaning (A and B) and after cleaning with an acetone (C and D). Evidence of loose and embedded filler fibers from the GFR-Bit can be seen on the composite surface (black arrow in B). What is not visible are fiber ends from the composite laminate (test panel). After cleaning, loose filler fibers have been removed but embedded fibers remain (black arrow in C) and fiber ends from the test panel laminate are visible (white arrow). This indicates Torlon from the bit smeared across the composite without damaging the composite test panel.

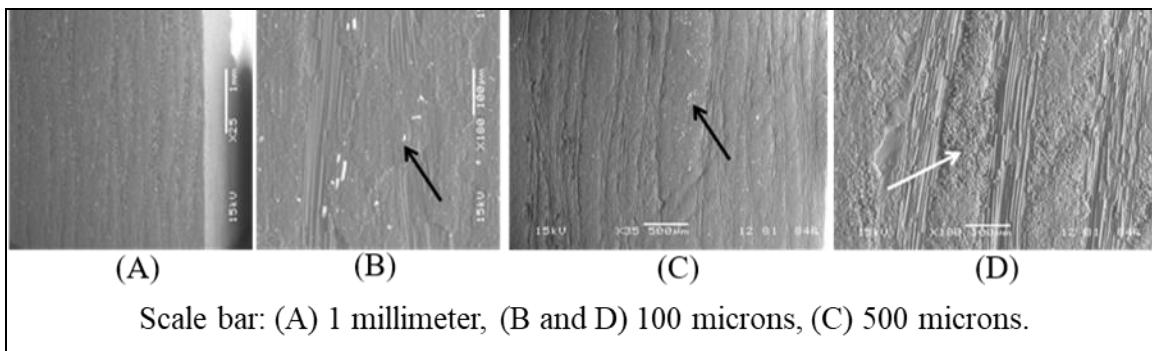


Figure 33. BMI Test Panel Gap Side Wall (Magnified)

The impinged test panel base, prior to cleaning (A) and after cleaning (B), is shown in Figure 34. GFR-Bit material can be seen on the impinged surface near the center of the images. Remnant Torlon was cleaned from one-half of the impinged area, as indicated by the arrow (B).

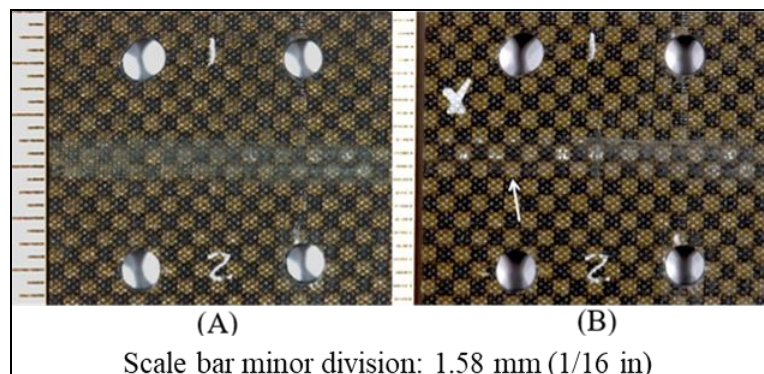


Figure 34. BMI Test Panel

The Figure 35 SEM images (A and B) show remnant GFR-Bit material (Torlon and fiberglass filler) on the surface of the impinged area, and images (C and D) show remnants of the material on the cleaned specimen.

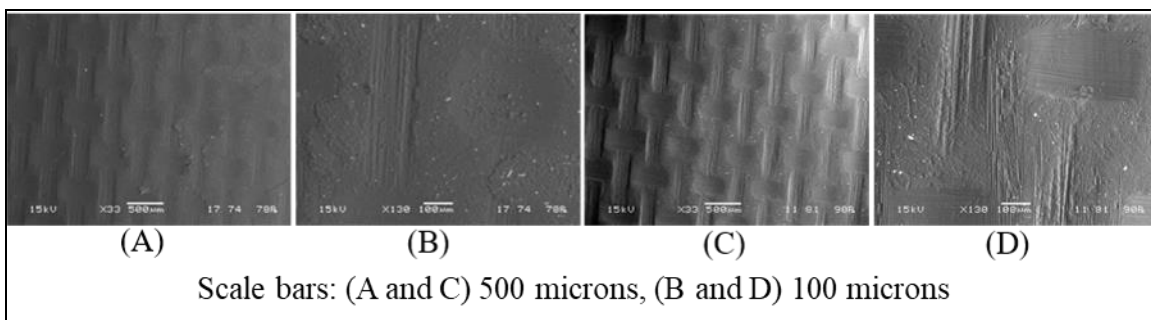


Figure 35. BMI Test Panel (Magnified)

Figure 36 shows evidence of slight wear (smearing) of a GFR-Bit used on the BMI test panel, indicated by the white arrow (A). Higher magnifications provided by the SEM images (B and C) reveal exposed Torlon 5030 filler fibers in the smeared area, indicated by the black arrow.

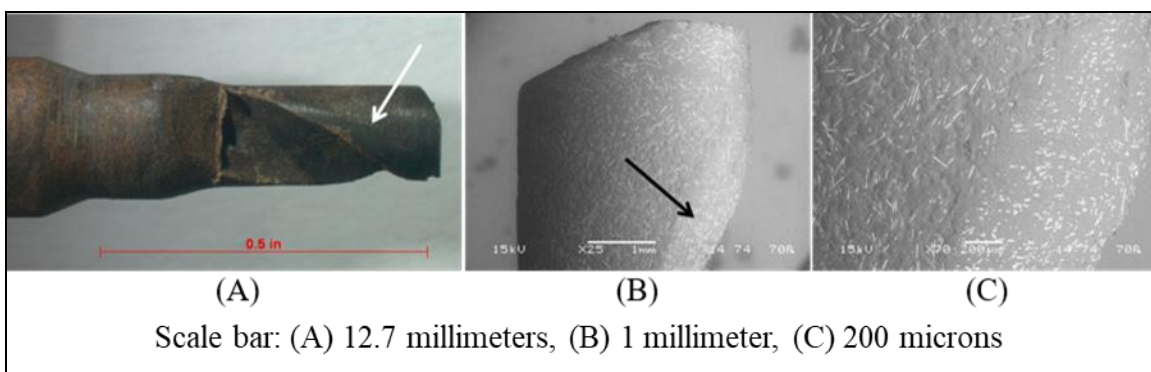


Figure 36. Torlon 5030 GFR-Bit Used on BMI Test Panel

Examination showed transfer of some Torlon 5030 GFR-Bit material to composite test panel surfaces but never any evidence of damage to the test panels. Simple cleaning using acetone on cotton swabs did not remove all transferred Torlon from composite test panels, but it is likely the small amount of transferred material remaining would be removed by subsequent surface preparation accomplished prior to reapplication of primer and gap filler, which typically includes abrasion as well as cleaning. Lastly, it is important to note activation of the GFR-Bit over a relatively small section of unprimed composite test panel for a period of 60 seconds, purposely attempting to damage the test panel, represents a more severe case than is expected to occur during normal usage of gap filler removal tools.

2.5 GFR-Bit (Final Article) Durability Trials and Demonstrations

Based on the combined results of the gap filler removal evaluations and panel damage evaluations, as well as a cost comparison of the bulk polymers, Torlon 5030 was identified as the likely material for full-rate GFR-Bit production. However, before proceeding with production, additional durability trials of longer duration were desired.

Utilizing composite test panels with machined grooves similar to those from the initial evaluations (Figure 16), GFR-Bits manufactured from Torlon 5030 were used to remove about 91 cm (3 ft) of gap filler as quickly as possible while running the 12,000 rpm Dotco grinder with line pressure in the 241 to 310 kPa (35-45 psi) range. This was done for both the old and new gap fillers. In this evaluation, a Torlon 5030 GFR-Bit removed a length of about 91 cm (3 ft) of the new gap filler in 3:34 (min:sec), and a GFR-Bit removed a similar length of the old gap filler in 4:45 (min:sec). Additionally, the wear observed on the bits was not significantly different than what was witnessed during the 30 cm (12 in) material removal trials when the GFR-Bits were operated at 172 kPa (25 psi) over this length.

Based on the success of the Torlon 5030 spiral single flute GFR-Bits during all evaluations, these bits were selected for full-scale production and commercialization.

3. TORLON SCRAPER BLADES (TSB)

Existing nonmetallic scraper blades are ineffective at removing most materials and dull quickly, requiring frequent re-sharpening or replacement. Several factors contribute to the tools' inadequacies, including their shapes, materials of composition, and general lack of rigidity. It was clear new scraper blade designs were required to efficiently removed materials without damaging underlying structure to minimize use of unapproved metallic tools on aircraft. Based on GFR-Bit evaluations, Torlon 5030 was chosen as the candidate material for new TSBs.

3.1 TSB Development

After examining the available nonmetallic material removal tools (Figure 1) and identifying their deficiencies, as well as studying the attributes of metallic tools that allowed successful removal of materials, five configurations of prototype TSBs were designed, as shown in Figure 37.

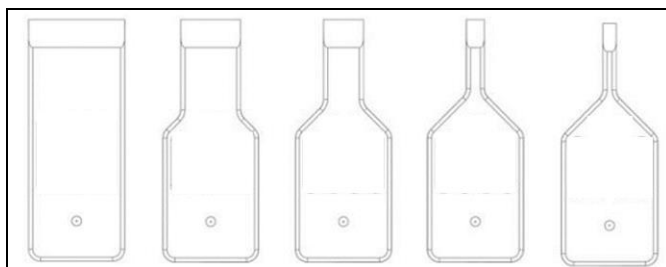


Figure 37. TSB Configurations

The key geometric feature of the TSB design is the 25°/25° asymmetrical 1/3-2/3 cutting tip (Figure 38). This feature, when used properly, eliminates the extreme pressure that must be placed on cutting edges for other tool designs and allows TSBs to better maintain their sharp cutting edges.

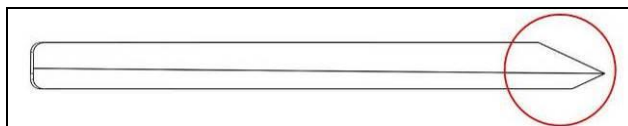


Figure 38. TSB's 25°/25° Asymmetrical 1/3-2/3 Cutting Tip

Prototype TSBs were machined from 6.35 mm (0.250 in) thick extruded Torlon 5030 sheet stock (Figure 39). Based on information provided by the injection molder and the manufacturer of the extruded materials, it was determined extruded sheet stock properties are similar to those of injection molded Torlon 5030. By machining prototype scraper blades from available extruded sheet, multiple scraper blade configurations could be evaluated at an accelerated rate and at much less cost than manufacturing an injection mold for each configuration. As an example, the cost of a part insert that could be placed in an existing injection mold base to produce a single TSB configuration is about \$8,000 compared to approximately \$70 to machine a single TSB from extruded sheet.

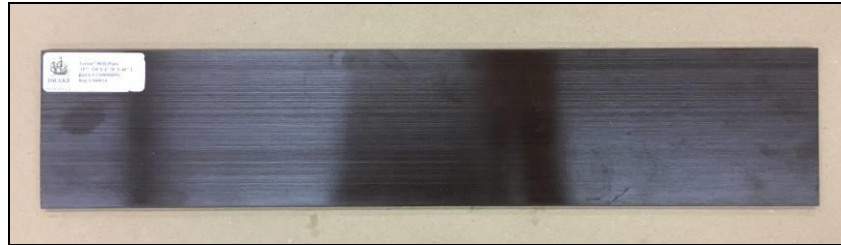


Figure 39. Torlon 5030 Extruded Sheet Stock

Accessories required to use TSBs and enhance their effectiveness were adapted or developed. These include handles, a pneumatic tool, and a fixture that ensures the 25°/25° asymmetrical 1/3-2/3 cutting tip is maintained during sharpening (Figure 40). The pneumatic tool is a modified gasket scraper fitted with a blade adapter designed to accommodate TSBs. Development work associated with the accessories is not discussed in this paper.



Figure 40. Commercially Available Injection Molded TSBs and Accessories

3.2 TSB Prototype Evaluation and Demonstration

Each TSB configuration was evaluated on a composite panel containing coating and tapes commonly found on aerospace vehicles. TSBs were mounted on a pneumatic tool connected to a 620.5 kPa (90 psi) compressed air source. With the TSB in contact with the material to be removed, the pneumatic tool was activated and slowly pushed through the material, as shown in Figure 41.

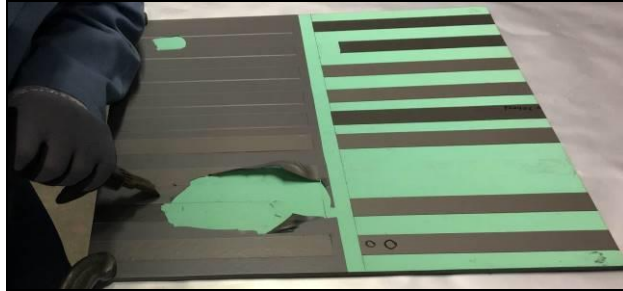


Figure 41. TSB Test Panel

Next, the TSBs were demonstrated at several repair depots and operational maintenance units (Figure 42) for additional feedback prior to manufacturing of injection molds and production of the injection molded TSB versions. As stated earlier, the machined TSB production cost is about \$70, whereas the injection molded TSB production cost is significantly less.



Figure 42. TSB Demonstration and Field Evaluation

3.3 Final Article Evaluation

For final article testing, injection mold bases and part inserts were manufactured, and the five final TSB configurations were produced, which included the following blade widths: 30.5 mm (1.2 in), 19 mm (0.75 in), 12.7 mm (0.5 in), 5.8 mm (0.23 in) and 4.3 mm (0.17 in). Results for the largest configuration (TSB-1200) are presented as a representative example (Figure 43). Torlon 5030 TSBs come out of the injection mold in a green state (not fully cured) and then receive a 21-day postcure at 260°C (500°F) to produce a final part. The postcure process darkens the material's color and increases TSB wear resistance and strength.



Figure 43. Injection Molded TSBs (TSB-1200)

The green stage and postcured injection molded TSBs were evaluated for part thickness variation and porosity concentration. A sampling of the injection molded TSBs were cross-sectioned for evaluation (Figure 44). No anomalies were observed.



Figure 44. Sectioned Injection Molded TSBs

To evaluate TSB-1200 bending strength, mechanical tests were performed using a three-point bending configuration with a 35.6 mm (1.4 in) span and a 3.2 mm (0.125 in) radius loading nose (Figure 45). The three-point bend test matrix and average peak loads obtained (minimum of five test specimens) are presented in Table 5.



Figure 45. TSB Three-Point Bend Test Setup

Table 5. Three-Point Bend Results for TSBs

Scraper Blade	Avg. Peak Load - kg (lbf)	Crosshead Displacement at Failure - mm (in)
Machined, Extruded Sheet Stock	744.7 (1642)	2.31 (0.091)
Injection Molded, Green Stage	124.7 (275)	0.58 (0.023)
Injection Molded, Postcured	424.1 (935)	1.49 (0.059)

Although the highest bending strength resulted from the machined sheet-stock, the postcured injection molded TSB-1200 configuration still has a higher bending strength than comparable nonmetallic material removal tools commercially available. Photographs of the failure modes are presented in Figure 46 - Figure 48.

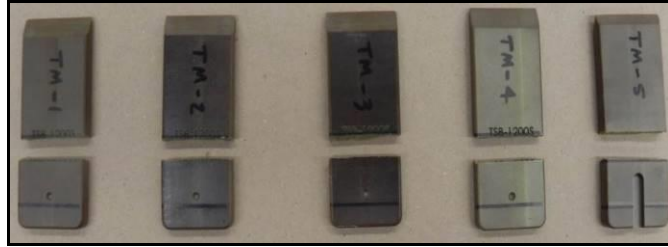


Figure 46. Machined TSBs



Figure 47. Green Stage Injection Molded TSBs

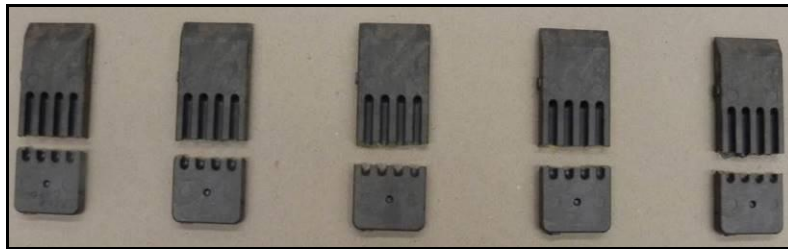


Figure 48. Postcured Injection Molded TSBs

The five widths of commercially available EnduroSharp TSBs were used with commercially available accessories and evaluated on both unprimed and primed carbon/epoxy composite test panels (Figure 49).

				
TSB 1200 (25°)	TSB 750 (25°)	TSB 500 (25°)	TSB 230 (25°)	TSB 170 (25°)
				
TSB 1200 (45°)	TSB 750 (45°)	TSB 500 (45°)	TSB 230 (45°)	TSB 170 (45°)
				
TSB 1200 (25°)	TSB 750 (25°)	TSB 500 (25°)	TSB 230 (25°)	TSB 170 (25°)
				
TSB 1200 (45°)	TSB 750 (45°)	TSB 500 (45°)	TSB 230 (45°)	TSB 170 (45°)

Figure 49. TSB Test Panels (25° and 45° Test Areas)

The TSBs were mounted on an EnduroSharp pneumatic tool (Part # ESPT001) operated at 620 kPa (90 psi), as shown in Figure 50. The evaluation consisted of multiple passes over twelve test areas on each test panel, with a tool angle of 25° to the surface maintained for a given blade on six test areas and a tool angle of 45° to the surface maintained for the other six.

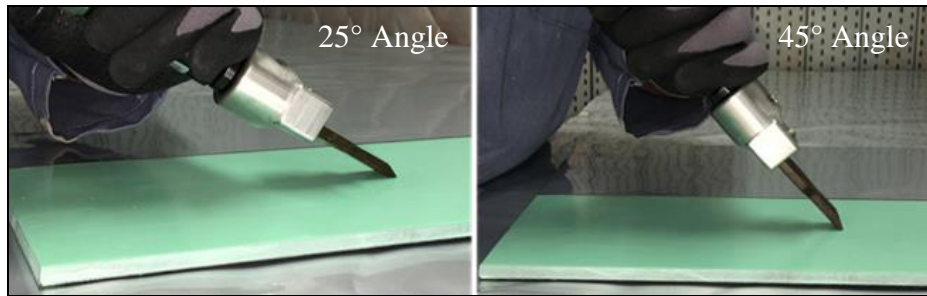


Figure 50. Mounted TSBs (25° and 45°)

Figure 51 shows the test areas of the unprimed carbon/epoxy composite test panels after testing. The panel was left unprimed to provide a worst case scenario, with the TSB in direct contact with the unprotected carbon/epoxy composite structure. Dashed boxes define test areas.

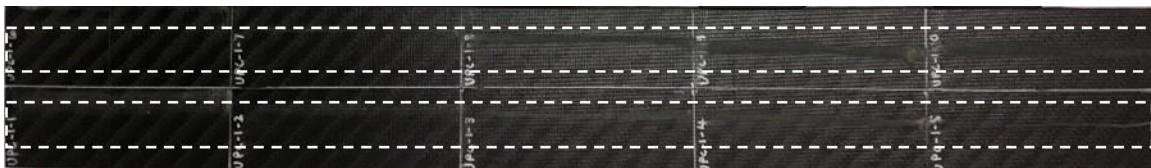


Figure 51. TSB Unprimed Test Panel Test Area (25° at the Top and 45° at the Bottom)

Table 6 provides details for the test process conducted on an unprimed carbon/epoxy composite test panel. Further information is provided below for specimens in the highlighted rows of the table. Force (last table column) was estimated by measuring applied force during material removal from sample specimens on a Cole-Parmer® scale (Symmetry PL-LBH-15K IS-Series).

Table 6. TSB Unprimed Test Panel Test Metrics

Panel ID	Specimen ID	Blade Style	Part Number	PSI	Blade Angle to Surface	Number of Passes	Elapsed Time (Seconds)	Test Area Length Millimeters (inches)	Force Kilograms (pounds)
UPC-1	UPC-1-1	TSB	TSB-1200	90	25°	6	15.85	31.8 x 88.9 (1.25 x 3.5)	4.8-6.0 (10.6-3.4)
UPC-1	UPC-1-2	TSB	TSB-750	90	25°	6	11.62	31.8 x 88.9 (1.25 x 3.5)	4.8 - 6.0 (10.6-13.4)
UPC-1	UPC-1-3	TSB	TSB-500	90	25°	6	11.93	31.8 x 88.9 (1.25 x 3.5)	4.8-6.0 (10.6-3.4)
UPC-1	UPC-1-4	TSB	TSB-230	90	25°	6	12.59	31.8 x 88.9 (1.25 x 3.5)	4.8-6.0 (10.6-3.4)
UPC-1	UPC-1-5	TSB	TSB-170	90	25°	6	13.22	31.8 x 88.9 (1.25 x 3.5)	4.8-6.0 (10.6-13.4)
UPC-1	UPC-1-6	TSB	TSB-1200	90	45°	6	17.42	31.8 x 88.9 (1.25 x 3.5)	5.1-6.6 (11.2-14.6)
UPC-1	UPC-1-7	TSB	TSB-750	90	45°	6	15.12	31.8 x 88.9 (1.25 x 3.5)	5.1-6.6 (11.2-14.6)
UPC-1	UPC-1-8	TSB	TSB-500	90	45°	6	12.71	31.8 x 88.9 (1.25 x 3.5)	5.1-6.6 (11.2-14.6)
UPC-1	UPC-1-9	TSB	TSB-230	90	45°	6	14.03	31.8 x 88.9 (1.25 x 3.5)	5.1-6.6 (11.2-14.6)
UPC-1	UPC-1-10	TSB	TSB-170	90	45°	6	13.01	31.8 x 88.9 (1.25 x 3.5)	5.1-6.6 (11.2-14.6)

Photo documentation of the test area from specimen UPC-1-1 of the unprimed test panel is provided in Figure 52 and is divided into three sections, as described below. The test consisted of six passes of a TSB-1200 at a 25° angle to the panel surface.

Section (1) of the figure shows the overall view of the test panel test area (right) and the TSB that passed across the test area (left). The green arrow identifies the portion of the TSB that made contact with the test panel surface. The regions of the test panel identified as “START” and “MIDDLE” indicate areas where the TSB began each pass and the midway point along each pass, respectively. These areas were removed for additional photo documentation, which is shown in section (2).

Section (2) images for the start (A) and middle (B) test areas were taken to the right of the yellow dots found on the section (1) image. Black arrows indicate increasing magnification. The red arrow in the highest-magnification image points to glass filler fibers from the TSB; no exposed test panel fibers were observed.

Section (3) provides SEM photomicrographs taken from the test area at locations indicated by the red arrows in the section (1) test area image, with (A) being a cross-sectional view of the test area at the start of a TSB pass across the test panel and (B) showing a cross-section taken from the test area near the midway point of the TSB pass. The spaces between the black arrows in these two cross-sectional images define the distance over which the TSB was in contact with test panel surface. The portion of (B) enclosed in the black box is shown in increased magnification in (C). As evidenced by the cross-sections, there were no cracks below the surface of the panel caused by TSB interaction with the surface.

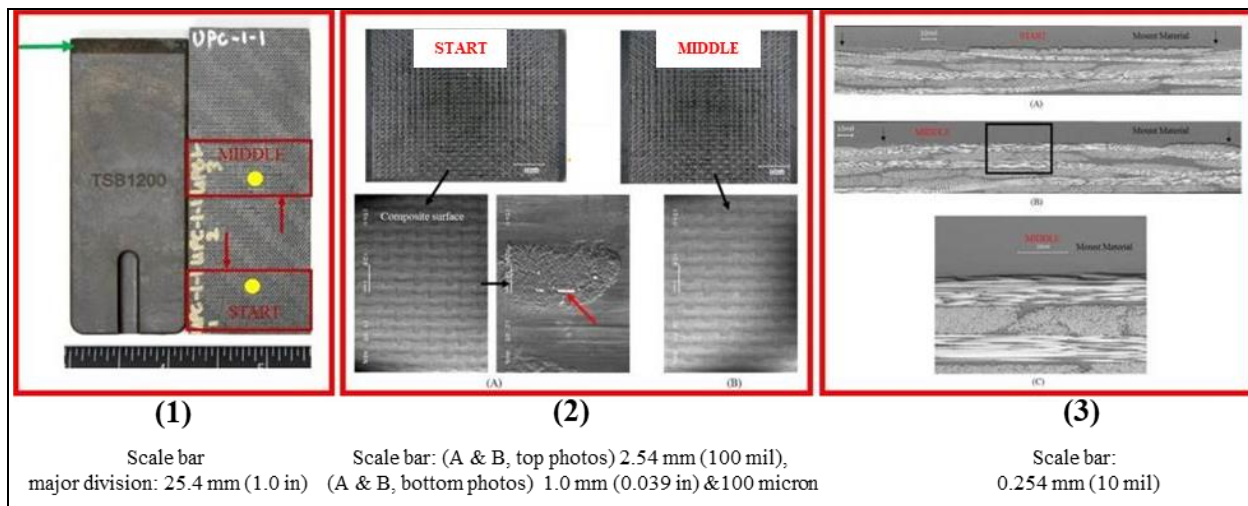


Figure 52. TSB-1200 (25°) Unprimed Test Panel Test Area

Figure 53 shows images of the TSB tested on Panel UPC-1-1 at an angle of 25° to the test panel surface. Image (A) provides an overall view of both sides of the blade. The green arrow indicates the location on the TSB from which the sample shown in (B) was taken, and the red arrow in (A) identifies the location on the tip of the TSB shown in the SEM image (C). The red arrow in (C) identifies the TSB surface that made contact with the composite test panel.

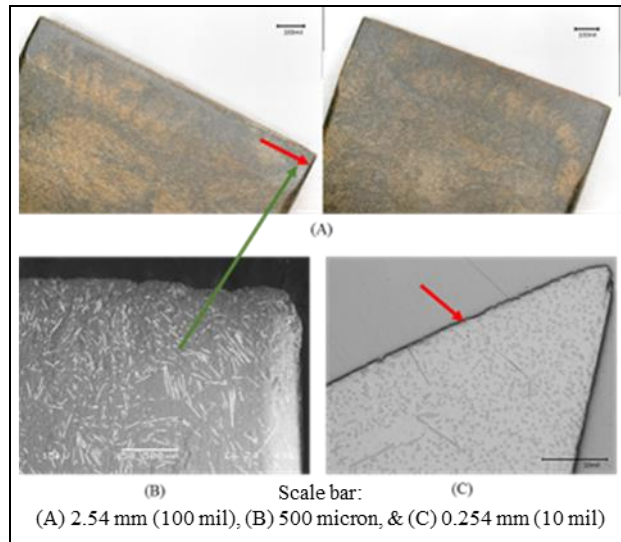


Figure 53. TSB-1200 (25°) after Use

As evidenced by the photographs, the TSB-1200 used at a 25° angle to surface during the six passes over the test panel was undamaged and received just a small amount of wear.

Photo documentation of the test area from specimen UPC-1-6 (see Table 6) is provided in Figure 54 and is divided into three sections similar to those described above for UPC-1-1. This test consisted of six passes of a TSB-1200 at a 45° angle to the panel surface. As was the case for specimen UPC-1-1, some fibers from the TSB were found on the test panel surface but no damage to the test panel was evident. Magnified views of the test area showed no exposed test panel fibers or subsurface cracks caused by TSB passes over the area.

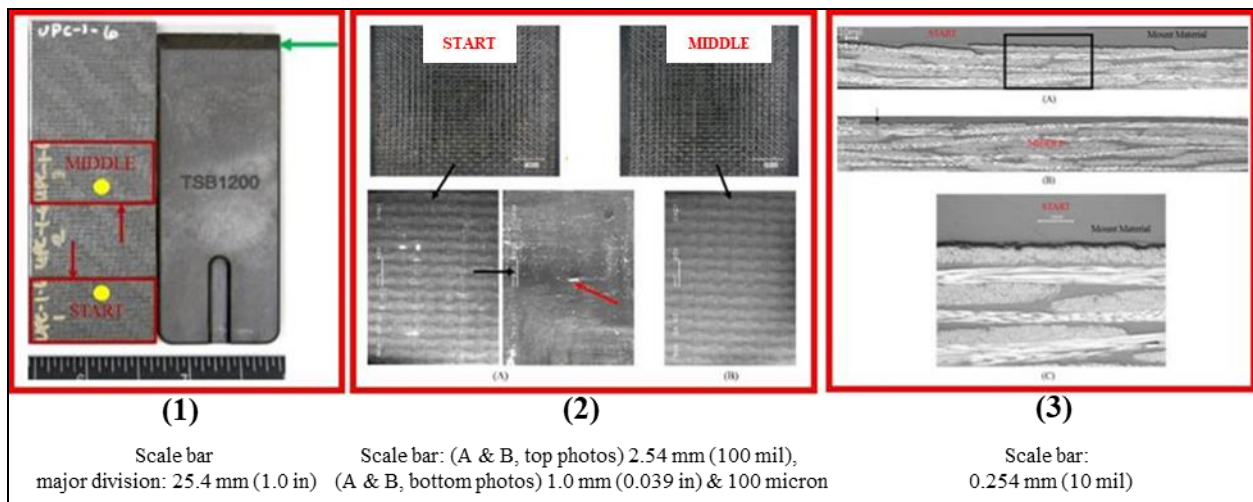


Figure 54. TSB-1200 (45°) Unprimed Test Panel Test Area

Figure 55 shows images of the TSB-1200 tested on Panel UPC-1-6 at an angle of 45° to the test panel surface. The various views and arrows are as described for Figure 53. Note the difference between this SEM image and the analogous image of the TSB used at a 25° angle on specimen UPC-1-1. In this case, deformation of the cutting edge due to the extreme angle at which the TSB contacted the panel surface is clearly evident.

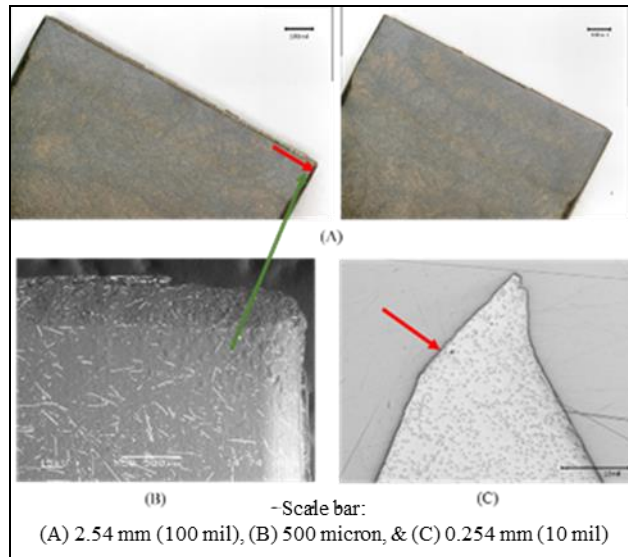


Figure 55. TSB-1200 (45°) after Use

Figure 56 shows the posttest areas on a carbon/epoxy composite test panel coated with a primer. The panel was primed to mimic an on aircraft structure and determine if material removal using TSBs will damage the primer. In the figure, black dashed boxes identify the test areas.

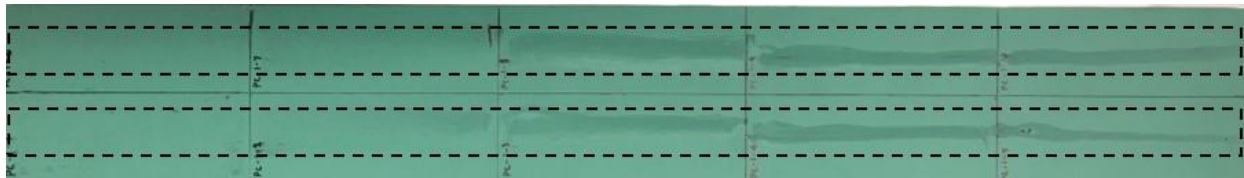


Figure 56. TSB Primed Test Panel Test Area (25° at the Top and 45° at the Bottom)

Table 7 provides details for the test process conducted on the primed carbon/epoxy composite test panel. Though similar data were generated for all specimens, further details are only provided for the four highlighted specimens. These include both tests (25° and 45° angles) using the largest blade, as well as two additional cases that generated results differing from the others. Force, provided in the last column of the table, was estimated using a Cole-Parmer scale in the same manner as was done for the analogous testing conducted on the unprimed test panel.

Table 7. TSB Primed Test Panel Test Metrics

Panel ID	Specimen ID	Blade Style	Part Number	PSI	Blade Angle to Surface	Number of Passes	Elapsed Time (Seconds)	Test Area Length Millimeters (inches)	Force Kilograms (pounds)
PC-1	PC-1-1	TSB	TSB-1200	90	25°	6	12.96	31.8 x 8.9 (1.25 x 3.5)	4.8-6.0 (10.6-3.4)
PC-1	PC-1-2	TSB	TSB-750	90	25°	6	11.32	31.8 x 8.9 (1.25 x 3.5)	4.8-6.0 (10.6-13.4)
PC-1	PC-1-3	TSB	TSB-500	90	25°	6	12.19	31.8 x 8.9 (1.25 x 3.5)	4.8-6.0 (10.6-13.4)
PC-1	PC-1-4	TSB	TSB-230	90	25°	6	12.40	31.8 x 8.9 (1.25 x 3.5)	4.8-6.0 (10.6-13.4)
PC-1	PC-1-5	TSB	TSB-170	90	25°	6	12.33	31.8 x 8.9 (1.25 x 3.5)	4.8 x 6.0 (10.6-13.4)
PC-1	PC-1-6	TSB	TSB-1200	90	45°	6	15.29	31.8 x 8.9 (1.25 x 3.5)	5.08-6.6 (11.2-14.6)
PC-1	PC-1-7	TSB	TSB-750	90	45°	6	13.37	31.8 x 8.9 (1.25 x 3.5)	5.08-6.6 (11.2-14.6)
PC-1	PC-1-8	TSB	TSB-500	90	45°	6	12.86	31.8 x 8.9 (1.25 x 3.5)	5.08-6.6 (11.2-14.6)
PC-1	PC-1-9	TSB	TSB-230	90	45°	6	12.82	31.8 x 8.9 (1.25 x 3.5)	5.08-6.6 (11.2-14.6)
PC-1	PC-1-10	TSB	TSB-170	90	45°	6	13.71	31.8 x 8.9 (1.25 x 3.5)	5.08-6.6 (11.2-14.6)

The photo documentation of the PC-1-1 test area shown in Figure 57 is divided in to three sections as was done for the UPC test specimens. The test consisted of six passes of the TSB-1200 at a 25° angle panel surface. As can be seen from the figure, no test panel fibers or TSB filler fibers were observed, and no cracks were seen below the test area surface. Minimal damage was done to the primer itself; some slight abrasion and remnant Torlon were present, but the primer was not penetrated.

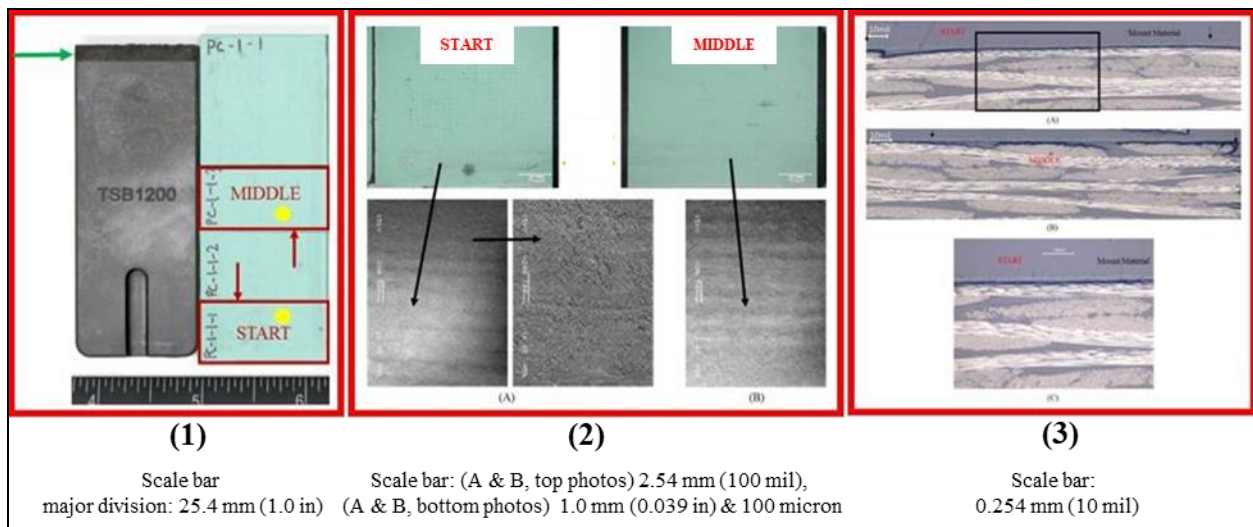


Figure 57. TSB-1200 (25°) Primed Test Panel Test Area

Figure 58 shows views of the TSB-1200 that was in contact with the test surface (25° angle). Details regarding the arrows are the same as for Figure 53 and Figure 55. Some wear can be seen on the TSB cutting edge, and the filler fibers can be observed under higher magnification.

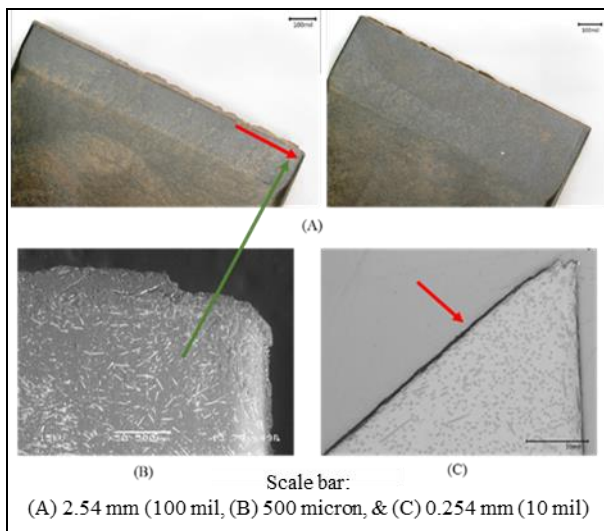


Figure 58. TSB-1200 (25°) after Use

The photo documentation of the PC-1-6 test area is shown in Figure 59. The figure is again divided into three sections as before. This test consisted of six passes of the TSB-1200 at a 45° angle to the panel surface. As was the case for the 25° angle test on the primed panel using a TSB-1200, minimal damage was done to the primer, which was not penetrated.

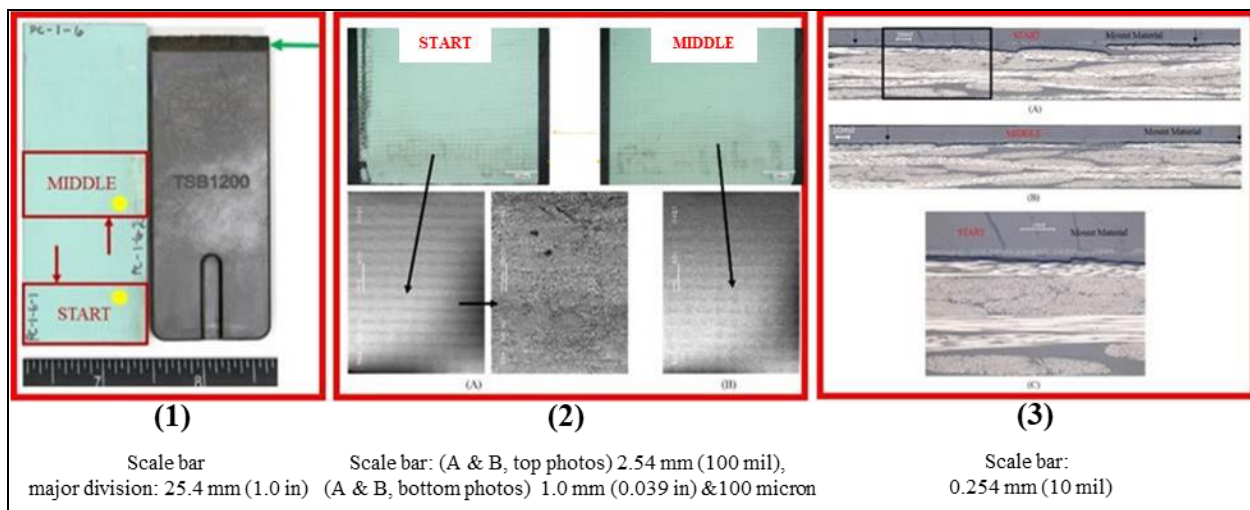


Figure 59. TSB-1200 (45°) Primed Test Panel Test Area

Figure 60, set up in the same manner as the previous TSB figures, shows the TSB-1200 that was in contact with the panel surfaces (45° angle). Note the slight deformation of the cutting edge due to the extreme angle as to which the TSB contacted the panel surface.

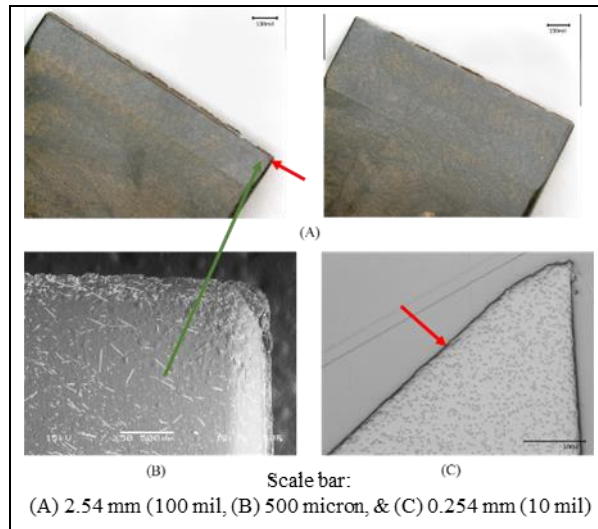


Figure 60. TSB-1200 (45°) after Use

The photo documentation in Figure 61 shows small areas of primer penetration, identified by the red circles. Test specimens PC-1-5 and PC-1-7, respectively, represent six passes with a TSB-170 used at a 25° angle and six passes with a TSB-750 used at a 45° angle. No damage to the underlying composite test panel was observed in either case. Though all results were not consistent since specimens PC-1-2 and PC-1-10 led to no penetration of the primer, the results do show the primer can be penetrated under some conditions. In no case was the composite material of the test panel damaged (i.e. no reinforcing fibers exposed and no matrix cracks generated).

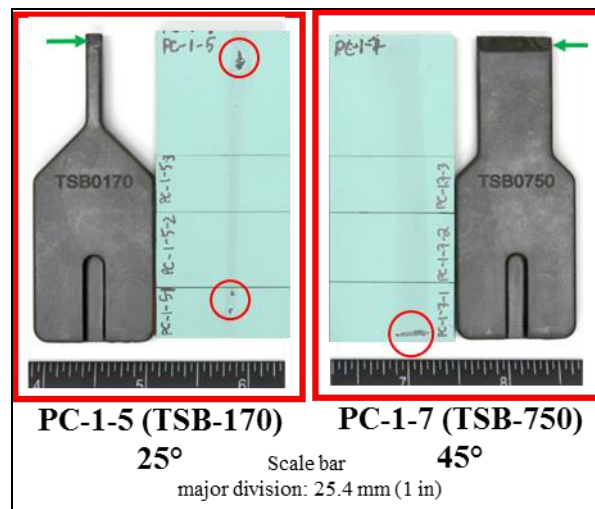


Figure 61. Damaged Primer

Based on the success of the in-house and external evaluations and demonstrations, full-scale production/commercialization of the five TSB configurations using Torlon 5030 material was sought. In addition, the associated accessories were also commercialized.

4. TORLON GAP BLADES (TGB)

Existing nonmetallic tools used for removing gap fillers are ineffective due to their designs, including material selection. The tools lack rigidity and dull quickly during use, requiring frequent re-sharpening or replacement. Designs of most commercially available nonmetallic gap filler removal tools have not been optimized to consider the properties of gap fillers themselves or the geometries of the structures from which the gap fillers must be removed. The GFR-Bits were optimized to remove specific flexibilized epoxy gap fillers, which are harder than polysulfide compounds used in most outer mold line gaps of aerospace vehicles. Polysulfide materials gum up GFR-Bits, causing them to fail after a few centimeters of gap filler removal.

The typical gap filler remover is a narrow-ended nonmetallic tool, similar to a scraper blade (Figure 62). The tool is sharpened at the tip, which is its only cutting surface. This type of design requires the tool to be plunged completely through the gap filler to the surface of the structure at the bottom of the gap (no depth control). The tool is then pushed through the gap, shearing the material at the interface between the gap filler and the underlying structure (bottom of the gap). Due to the lack of cutting surfaces on the sides of the tool, gap filler adhered to the sides of the gap must be ripped from those surfaces via brute force. In some instances, to ease the removal process, aircraft maintainers use a traditional metal razor blade to separate gap filler from the sides of the gap, potentially damaging the structure, prior to using nonmetallic gap filler removal tools. Also, due to the lack of robust and effective gap filler removal using the existing scraper-like tools, maintainers often employ unapproved metallic tools (Figure 2).



Figure 62. Examples of Available Gap Filler Removal Tools

In an effort to eliminate or minimize the use of metallic tools on aircraft structures for gap filler removal, including removal of polysulfide materials, it was clear a new removal tool design was required. Based on the material evaluations conducted during development of the GFR-Bits, Torlon 5030 was chosen as the candidate material for new TGBs.

4.1 TGB Development

As was the case for GFR-Bit development, available ineffective nonmetallic gap filler removal tools were evaluated, identifying their deficiencies, and the attributes of unauthorized metallic tools that allowed them to be successful in material removal were also studied. The design

concept, shown in Figure 63, consists of replaceable blades of varying widths and depths along with an adapter that enables use with the handles and pneumatic tool adopted for TSBs.

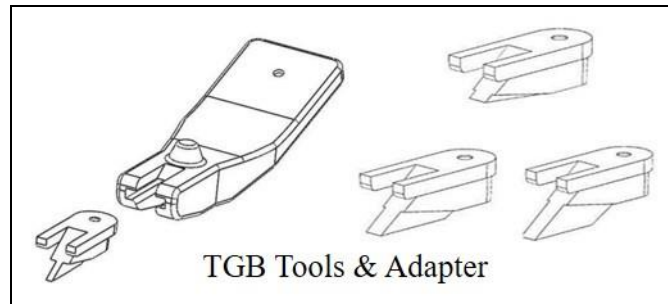


Figure 63. TGB and Adapter Designs

Three cutting edges were designed into the TGBs. These edges at the tip and along the sides of the cutting surface were designed to shear gap filler rather than rip it using brute force, providing an easier and faster transition through the filled gap and quicker gap filler removal.

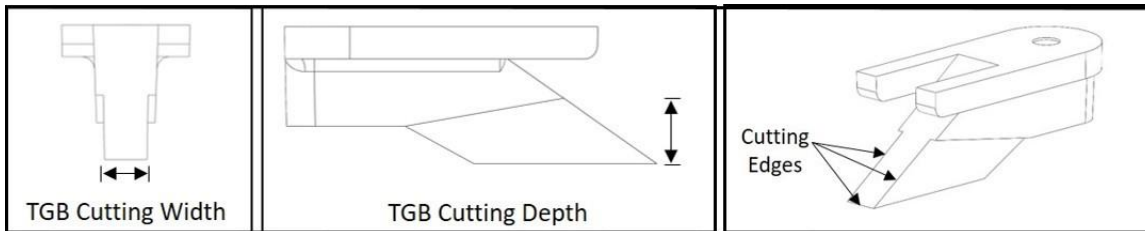


Figure 64. TGB Cutting Features

The TGB design was based on a commercially available metallic sheet metal ripper, which is shown in Figure 65 alongside prototype TGBs and adapters.



Figure 65. Sheet Metal Ripper with Prototype TGBs and Adapters

Prototype TGBs were machined from a 12.7 mm (0.50 in) thick extruded Torlon 5030 sheet, and the adapter was machined from 25.4 mm (1.0 in) thick unfilled DuPont™ Delrin® thermoplastic.

Commercialized (injection molded) TGBs and accessories are shown in Figure 66. The blades are available in five widths: 1.9 mm (0.075 in), 2.5 mm (0.10 in), 3.05 mm (0.12 in), 4.3 mm (0.17 in) and 5.8 mm (0.23 in). Each blade width is available in three cutting depths: 1.9 mm (0.075 in), 4.1 mm (0.16 in) and 6.35 mm (0.25 in). The multiple depths allow for incremental

removal of gap filler, starting with the shallowest-depth blade and followed by the other two depths, as needed. This technique eases removal and can reduce removal time even though multiple blades are used.



Figure 66. TGBs and Accessories

4.2 TGB Prototype Evaluation and Demonstration

Each machined prototype TGB configuration was evaluated on a composite panel containing coating and tapes commonly found on aerospace vehicles. TGBs were inserted into the holder adapter which was designed such that it could fit the same modified pneumatic tool used with TSBs. The pneumatic tool was connected to a 620 kPa (90 psi) compressed air source and, with the TGB in contact with the gap filler to be removed, the pneumatic tool was activated and slowly pushed through the gap filler (Figure 67).

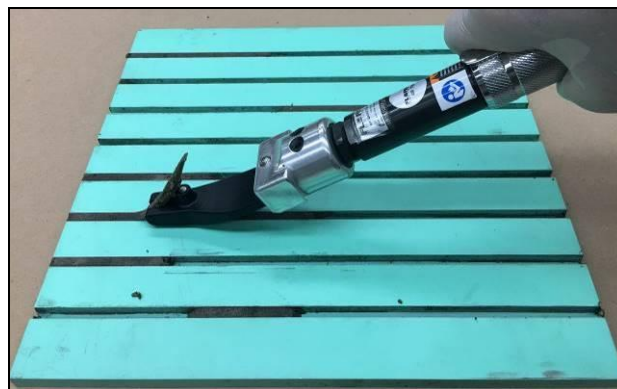


Figure 67. TGB Test Panel

As with the TSBs, the next step was to demonstrate TBGs at several repair depots and operational maintenance units (Figure 42) for additional feedback prior to the manufacturing of molds and parts inserts for production of injection molded TGBs.

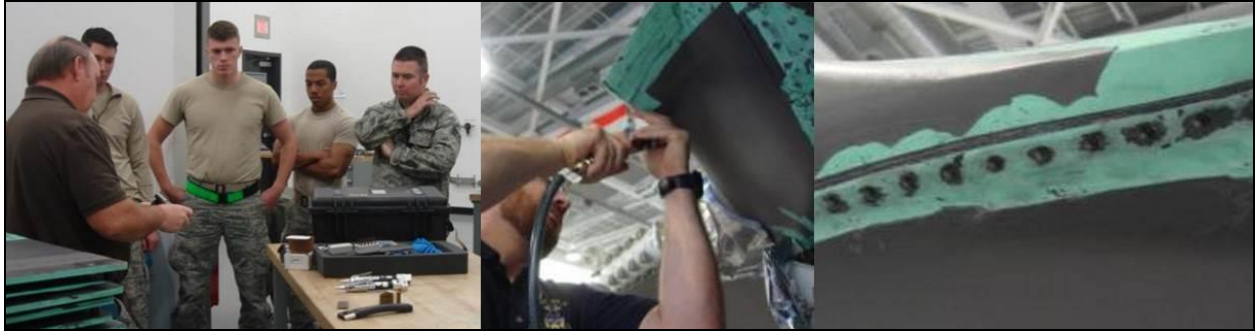


Figure 68. TGB Demonstration and Field Evaluation

4.3 TGB Final Article Evaluation

For the final article testing, injection mold bases and parts inserts were manufactured and TGBs (five widths, each having three depths) were produced. For illustrative purposes, only the largest blade will be discussed. This TGB-23-25 has the 5.8 mm (0.23 in) width and 6.35 mm (0.25 in) cutting depth. Figure 69 shows green stage and postcured TGBs of this configuration.

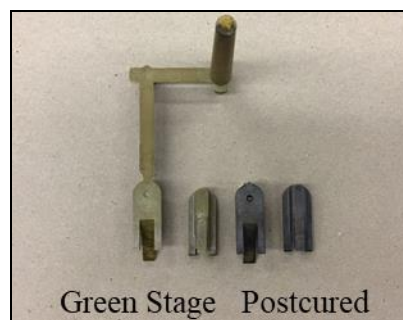


Figure 69. Injection Molded TGBs (TGB-23-25)

The green stage and postcured injection molded TGBs were evaluated for part thickness variation and porosity concentration. A sampling of the injection molded TGBs were cross-sectioned for evaluation (Figure 70). No anomalies were observed.



Figure 70. Sectioned Injection Molded TGBs (Green Stage)

Using commercially available blades and accessories, the five widths of TGB with the greatest cutting depth (TGB-xx-25) were evaluated on both unprimed and primed carbon/epoxy composite test panels (Figure 71). These panels were similar to those fabricated for GFR-Bit evaluation, with composite strips fastened to a composite material base, creating simulated gaps. In this case, gap widths were sized to fit the five TGB widths. For each test, the TGB holder

adapter with designated blade was mounted to an EnduroSharp pneumatic tool operated at 620 kPa (90 psi), as shown in Figure 71. Evaluations consisted of a single pass trial and a six-pass trial (in two separate gaps) for each of the five TGB widths, creating 10 total TGB test areas on the test panel.

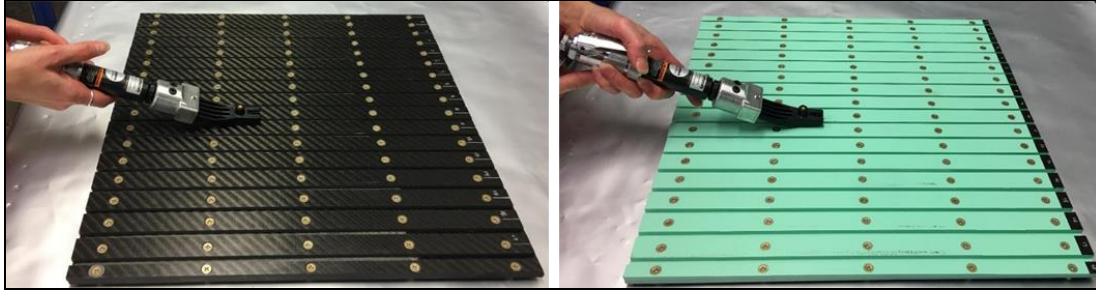


Figure 71. TGB Test Panel Damage Evaluation

Figure 72 shows overall views of the Unprimed Unfilled Gap Composite-1 (UPUFGC-1) panel both pretest (left image in figure) and posttest (image on right), which shows only the composite base after removal of the composite strips that formed the side walls of the simulated gaps. The panel was unprimed to provide a worst case scenario; TGBs were in direct contact with the unprotected carbon/epoxy composite structure. The numbers at the top of the panel identify gaps, which are immediately to the right of their respective number. Not all test panel simulated gaps were used for the TGB evaluation. Some gaps were left in pristine condition to create separation between the test areas used for each width blade. Also, the two test areas to the far left of the panel were used for GFR-Discs, which are not discussed in this paper. The red boxes in the figure identify the region of the test panel used for the TGB evaluation. The white lines on the panel after testing are remnant Torlon material from the TGBs.

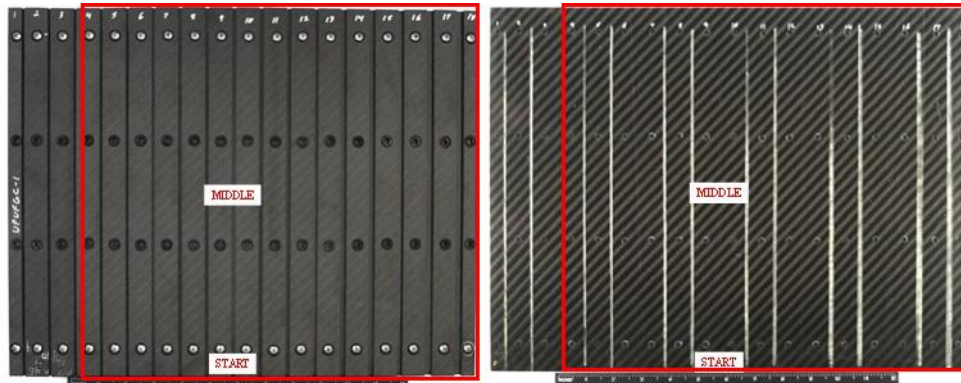


Figure 72. UPUFGC-1 Test Panel Pretest and Posttest (Disassembled)

Table 8 provides details for the tests conducted on the unprimed carbon/epoxy composite test panel. The table associates the gap identification numbers found on the panel with each test. Similar to TSB tests, the force value shown in the last table column was estimated by measuring applied force during material removal from sample specimens on a Cole-Parmer® scale (Symmetry PL-LBH-15K IS-Series). Tests conducted using the TGB-23-25, which is the largest blade (width and depth), are highlighted in yellow in the table. Further information for these two

tests is provided below the table. Test results for TGB-23-25 are similar to those generated for the other TGB configurations.

Table 8. TGB Unprimed Test Panel Damage Evaluation Test Metrics

Panel ID	Gap ID	Blade Style	Part Number	Disc/Blade Thickness mm (in)	Blade Depth mm (in)	Gap Width mm (in)	Gap Depth mm (in)	kPa (psi)	Number of Passes	Elapsed Time (Seconds)	Gap Length cm (in)	Force kg (lbs)
UPUFGC-1	4	TGB	TGB-75-25	19.05 (0.075)	6.35 (0.250)	2.41 (0.095)	4.88 (0.192)	620.5 (90)	1	13.92	30.5 (12.0)	1.59-2.27 (3.5-5.0)
UPUFGC-1	5	TGB	TGB-75-25	19.05 (0.075)	6.35 (0.250)	2.41 (0.095)	4.88 (0.192)	620.5 (90)	6	25.22	30.5 (12.0)	1.59-2.27 (3.5-5.0)
UPUFGC-1	7	TGB	TBG-10-25	2.54 (0.100)	6.35 (0.250)	3.05 (0.120)	4.88 (0.192)	620.5 (90)	1	13.95	30.5 (12.0)	1.59-2.27 (3.5-5.0)
UPUFGC-1	8	TGB	TBG-10-25	2.54 (0.100)	6.35 (0.250)	3.05 (0.120)	4.88 (0.192)	620.5 (90)	6	19.47	30.5 (12.0)	1.59-2.27 (3.5-5.0)
UPUFGC-1	10	TGB	TGB-12-25	3.05 (0.120)	6.35 (0.250)	3.56 (0.140)	4.88 (0.192)	620.5 (90)	1	12.18	30.5 (12.0)	1.59-2.27 (3.5-5.0)
UPUFGC-1	11	TGB	TGB-12-25	3.05 (0.120)	6.35 (0.250)	3.56 (0.140)	4.88 (0.192)	620.5 (90)	6	23.42	30.5 (12.0)	1.59-2.27 (3.5-5.0)
UPUFGC-1	13	TGB	TGB-17-25	4.32 (0.170)	6.35 (0.250)	4.83 (0.190)	4.88 (0.192)	620.5 (90)	1	15.48	30.5 (12.0)	1.59-2.27 (3.5-5.0)
UPUFGC-1	14	TGB	TGB-17-25	4.32 (0.170)	6.35 (0.250)	4.83 (0.190)	4.88 (0.192)	620.5 (90)	6	24.28	30.5 (12.0)	1.59-2.27 (3.5-5.0)
UPUFGC-1	16	TGB	TGB-23-25	5.85 (0.230)	6.35 (0.250)	6.35 (0.250)	4.88 (0.192)	620.5 (90)	1	14.67	30.5 (12.0)	1.59-2.27 (3.5-5.0)
UPUFGC-1	17	TGB	TGB-23-25	5.85 (0.230)	6.35 (0.250)	6.35 (0.250)	4.88 (0.192)	620.5 (90)	6	28.22	30.5 (12.0)	1.59-2.27 (3.5-5.0)

Photo documentation of the UPUFGC-1 Gap #16 test area shown in Figure 73 is divided into three sections. The test consisted of one pass of a TGB-23-25 through the full length of the gap, with the TGB parallel to the bottom of the gap and in contact with the base composite panel surface (bottom of the simulated gap).

Section (1) in the figure shows an overall view of the panel base in the test area after disassembly (top image) and provides views of the TGB used during the test, which is the blade in the red circle on the right. The two horizontal white lines in the top image are remnant Torlon from the TGB. The line at the bottom in this image is the one associated with this test (single pass).

In Section (2), photos show increased-magnification views of the test panel's test area near the middle of the TBG pass over its surface (A) and near the start of the pass (B). Black arrows indicate increasing magnification. The red arrow in the highest-magnification image identifies filler fibers from the TGB. There is no evidence of exposed carbon fibers from the test panel or any other type of damage to the panel.

Section (3) of the figure shows a cross-sectional image of the test panel at a location near the start of the TGB pass across the test area (A) and another cross-section near the midway point of the TGB pass (B). The location for the increased magnification image (C) is shown by the black box in (A). No matrix cracking or other damage was seen in the composite test panel.

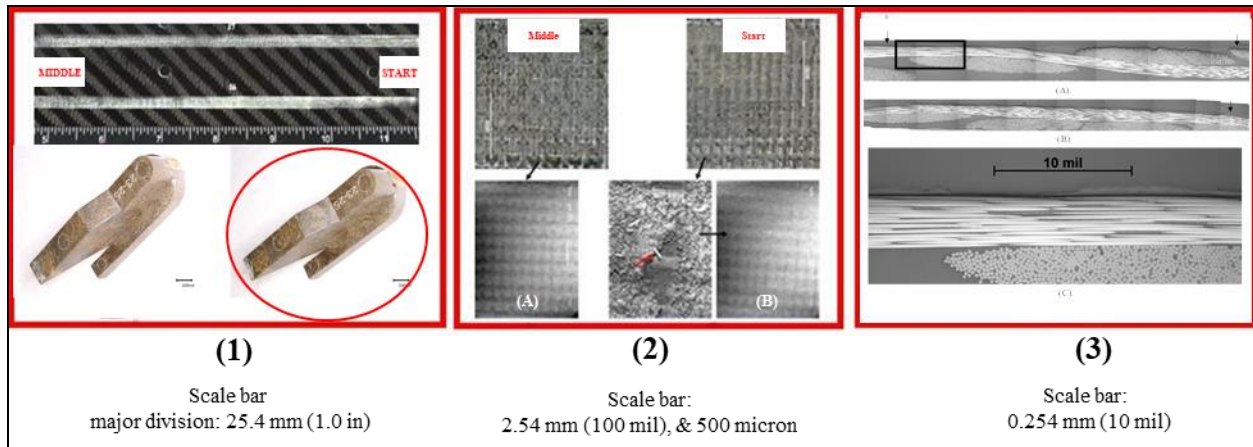


Figure 73. Test Panel UPUFGC-1, Gap #16

Figure 74 provides images of the TGB used during the test, which is shown in the red circle in Figure 73. The macroscopic view reveals some abrasion marks (A). An SEM image of the cutting edge (B) shows no evidence of carbon fibers from the test panel. A cross-sectional view of the cutting tip shows no evidence of carbon fibers from the test panel and little blade wear. The red arrows point to the same surface (A and C). These TGB images indicate no damage to the composite test panel during this test and little effect on the TGB.

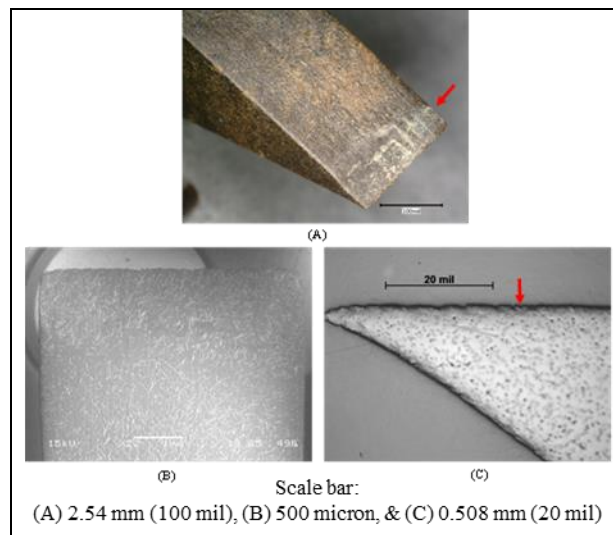


Figure 74. TGB-23-25 after One Pass

Photo documentation of the UPUFGC-1 Gap #17 test area is shown in Figure 75 and divided into three sections. The test consisted of six passes of a TGB-23-25 through the full length of the gap, with the TGB parallel to the bottom of the gap and in contact with the base composite panel surface (bottom of the simulated gap). The three sections in the figure are analogous to those found in Figure 73, with the images in first sections of the two figures being identical. For this test, the blade used is shown on the left side (in a red circle), and the upper horizontal line in the top image is remnant Torlon material left by the TGB on the panel. In Section (2) of the figure, the red arrow locates filler fiber from the TGB left on the test panel surface. The images show no evidence of damage to the test panel (no exposed composite panel fibers or matrix cracking).

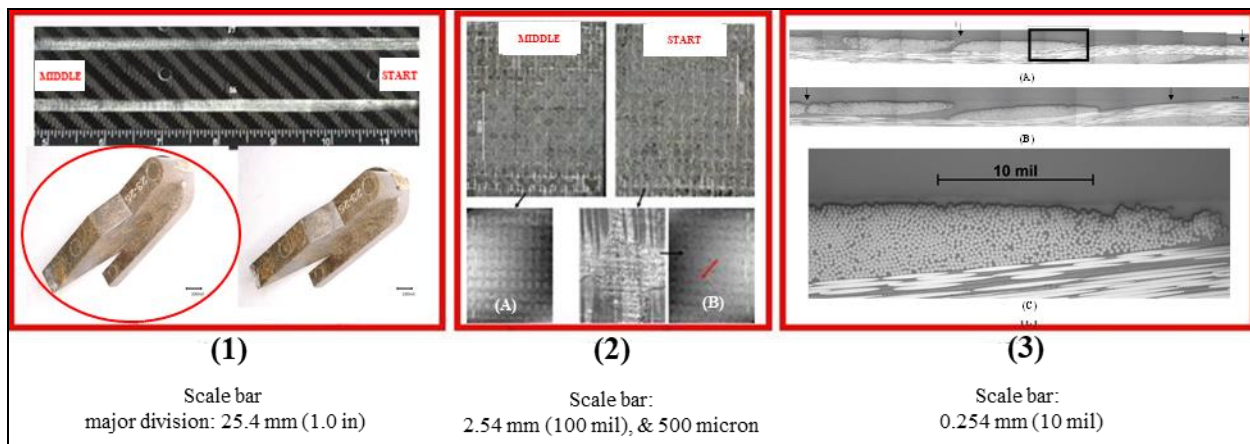


Figure 75. Test Panel UPUFGC-1, Gap #17

Figure 76 for Gap #17 (six passes using a TGB-23-25) is analogous to Figure 73. No evidence of carbon fibers from the test panel are seen on the blade. Slight abrasion of the blade can be seen, but very little wear occurred.

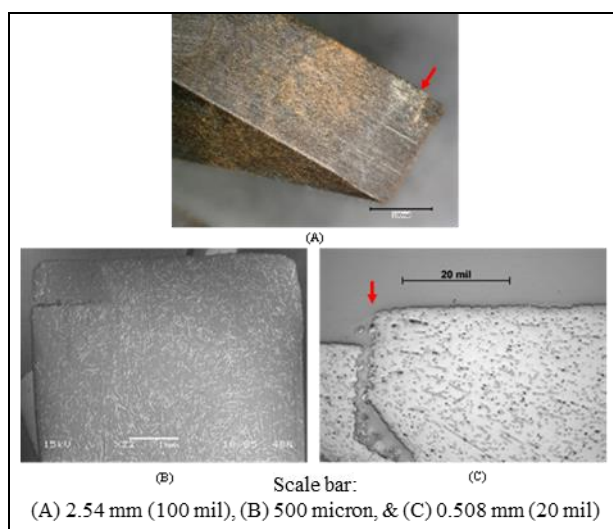


Figure 76. TGB-23-25 after Six Passes

Figure 77 shows overall view of the Primed Unfilled Gap Composite-1 (PUFGC-1) panel both pretest (left image in figure) and posttest (image on right), which shows only the composite base after removal of the composite strips that formed the side walls of the simulated gaps. Primer was applied to the panel to mimic an on-aircraft structure and determine if TSBs will damage the primer during the gap filler removal process. The numbers at the top of the panel identify gaps, which are immediately to the right of their respective number. As was the case for the unprimed test panel, not all simulated gaps were used for the TGB evaluation. The red boxes in the figure identify the region of the test panel used for the TGB evaluation. The streaks visible on the panel after testing are remnant Torlon material from the TGBs.

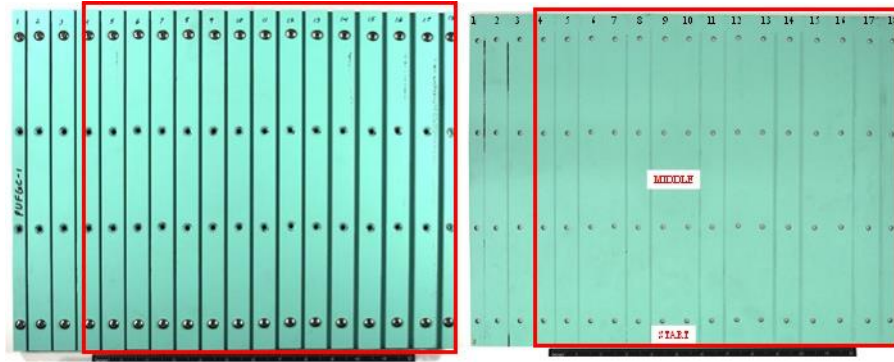


Figure 77. Primed Unfilled Gap Composite (PUFGC-1) Test Panel

Table 9 provides details for the tests conducted on the primed carbon/epoxy composite test panel. The table associates the gap identification numbers found on the panel with each test. AS before, force values shown (last table column) were estimated using the Cole-Parmer scale. Additional data are provided below the table for TGB-23-25 tests, highlighted in yellow in the table. Results from these tests are representative of those for the other TBG configurations.

Table 9. TGB Primed Test Panel Damage Evaluation Test Metrics

Panel ID	Gap ID	Blade Style	Part Number	Disc/Blade Thickness mm (in)	Blade Depth mm (in)	Gap Width mm (in)	Gap Depth mm (in)	kPa (psi)	Number of Passes	Elapsed Time (Seconds)	Gap Length cm (in)	Force kg (lbs)
PUFGC-1	4	TGB	TGB-75-25	19.05 (0.075)	6.35 (0.250)	2.41 (0.095)	4.88 (0.192)	620.5 (90)	1	6.89	30.5 (12.0)	1.59-2.27 (3.5-5.0)
PUFGC-1	5	TGB	TGB-75-25	19.05 (0.075)	6.35 (0.250)	2.41 (0.095)	4.88 (0.192)	620.5 (90)	6	27.03	30.5 (12.0)	1.59-2.27 (3.5-5.0)
PUFGC-1	7	TGB	TGB-10-25	2.54 (0.100)	6.35 (0.250)	3.05 (0.120)	4.88 (0.192)	620.5 (90)	1	10.50	30.5 (12.0)	1.59-2.27 (3.5-5.0)
PUFGC-1	8	TGB	TGB-10-25	2.54 (0.100)	6.35 (0.250)	3.05 (0.120)	4.88 (0.192)	620.5 (90)	6	25.42	30.5 (12.0)	1.59-2.27 (3.5-5.0)
PUFGC-1	10	TGB	TGB-12-25	3.05 (0.120)	6.35 (0.250)	3.56 (0.140)	4.88 (0.192)	620.5 (90)	1	10.14	30.5 (12.0)	1.59-2.27 (3.5-5.0)
PUFGC-1	11	TGB	TGB-12-25	3.05 (0.120)	6.35 (0.250)	3.56 (0.140)	4.88 (0.192)	620.5 (90)	6	21.26	30.5 (12.0)	1.59-2.27 (3.5-5.0)
PUFGC-1	13	TGB	TGB-17-25	4.32 (0.170)	6.35 (0.250)	4.83 (0.190)	4.88 (0.192)	620.5 (90)	1	12.68	30.5 (12.0)	1.59-2.27 (3.5-5.0)
PUFGC-1	14	TGB	TGB-17-25	4.32 (0.170)	6.35 (0.250)	4.83 (0.190)	4.88 (0.192)	620.5 (90)	6	23.90	30.5 (12.0)	1.59-2.27 (3.5-5.0)
PUFGC-1	16	TGB	TGB-23-25	5.85 (0.230)	6.35 (0.250)	6.35 (0.250)	4.88 (0.192)	620.5 (90)	1	11.23	30.5 (12.0)	1.59-2.27 (3.5-5.0)
PUFGC-1	17	TGB	TGB-23-25	5.85 (0.230)	6.35 (0.250)	6.35 (0.250)	4.88 (0.192)	620.5 (90)	6	25.33	30.5 (12.0)	1.59-2.27 (3.5-5.0)

Photo documentation of the PUFGC-1 Gap #16 test area shown in Figure 78 is divided in to three sections, which are set up in the same fashion as those for the analogous testing on the unprimed panel (Figure 73). The test consisted of one pass of a TGB-23-25 through the full length of the gap with the TGB parallel to the bottom of the gap and in contact with the base composite panel surface (bottom of the simulated gap). This pass, using the TGB shown in the red circle in the figure, shows some abrasion of the primer and is associated with the lower horizontal line found in the top image in Section (1) of the figure. Penetration of the primer only

occurred in a very small area that is hardly noticeable (see red circle) in the Section (1) image but can be seen under high magnification in Section (2) associated with the test area near the start of the TGB pass across the surface (B). The SEM image of this small area shows no composite test panel damage. In fact, there are no indications of damage to the composite test panel in any area (no exposed carbon fibers or matrix resin cracks).

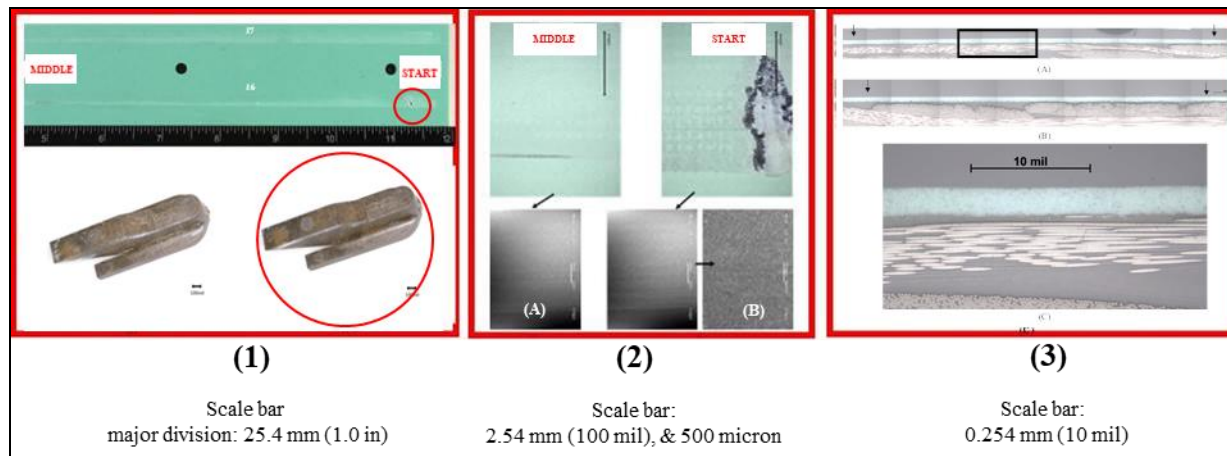


Figure 78. Test Panel PUFGC-1, Gap #16

Figure 79 shows images of the TGB-23-25 used for the test. Explanation for the figure is the same as that provided for similar figures generated for data from the unprimed panel tests. As before, no evidence of carbon fibers from the test panel can be found on the TGB, which shows little wear.

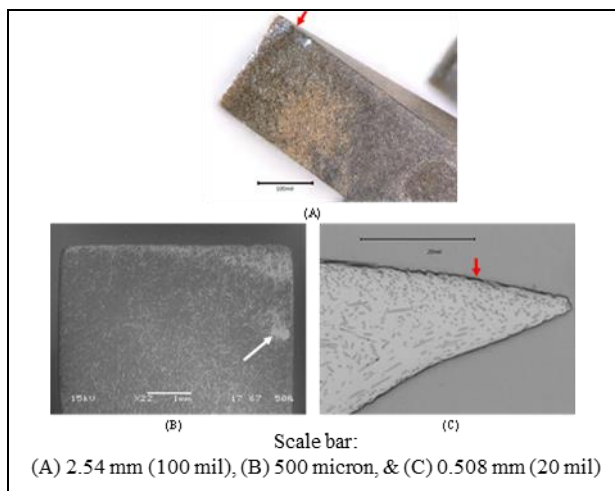


Figure 79. TGB-23-25 after One Pass

Photo documentation of the PUFGC-1 Gap #17 test area is provided in Figure 80 and is divided into the same three sections as before. The test consisted of six passes of a TGB-23-25 through the full length of the gap, with the TGB parallel to the bottom of the gap and in contact with the base composite panel surface (bottom of the simulated gap). This test, using the TGB shown in the red circle in the figure, shows some abrasion of the primer but no penetration of the primer,

and the test pass is associated with the upper horizontal line found in the top image in Section (1) of the figure.

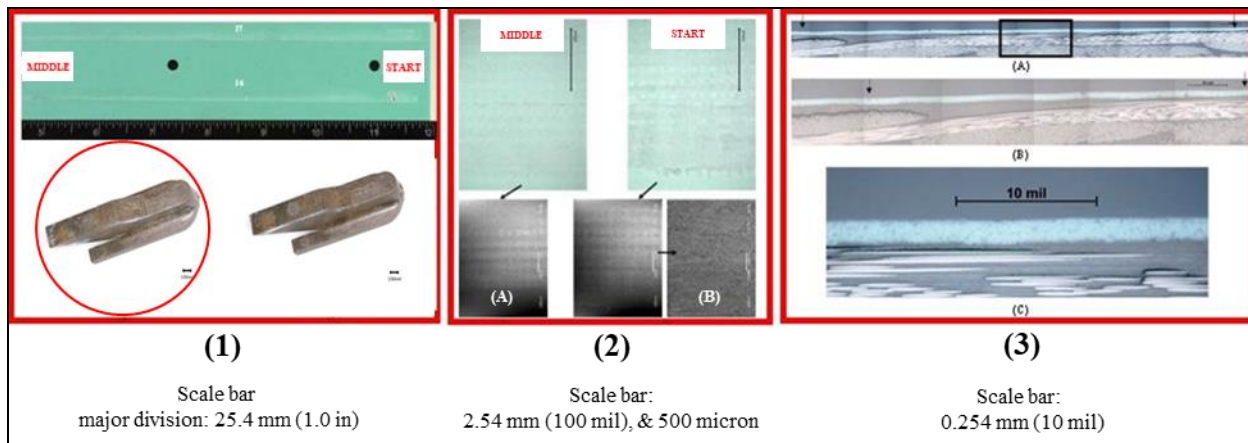


Figure 80. Test Panel UPUFGC-1, Gap #17

Figure 81 shows images of the TGB-23-25 used for the test. As before, no evidence of carbon fibers from the test panel can be found on the TGB, which shows little wear.

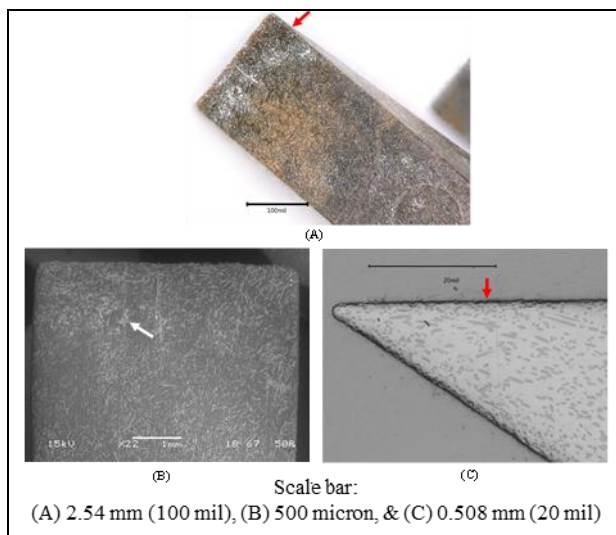


Figure 81. TGB-23-25 after Six Passes

5. CONCLUSIONS

AFRL and UDRI developed several new material removal tools intended to reduce use of unapproved metallic tools that can damage aircraft structure. These GFR-Bits, TSBs, and TGBs are manufactured from Torlon 5030 (fiberglass reinforced PAI) and provide aerospace maintainers more efficient methods for removing elastomeric coatings, gap fillers, boots, tapes, sealants, and PSA residue without causing damage to underlying fiber-reinforced composite structure. Their unique designs and Torlon 5030 composition, coupled with proper usage techniques, enable GFR-Bits, TSBs, and TGBs to be highly efficient and durable material

removal tools. They maintain cutting edges better than other nonmetallic removal tools and are easy to re-sharpen using sand paper. Torlon 5030 provides high strength and stiffness up to 260°C (500°F), as well as resistance to common aircraft fluids and maintenance chemicals.

The AFRL/UDRI-developed GFR-Bits, TSBs and TGBs are now commercially available from Performance Plastics, LTD (Cincinnati, OH) under the EnduroSharp trade name. The EnduroSharp removal tools have been evaluated and approved for applications on multiple aerostructures and have several industrial applications as well.



Figure 82. EnduroSharp™ Nonmetallic Material Removal Tools

6. ACKNOWLEDGEMENTS

6.1 Acknowledgements

This work was conducted under USAF contract FA8650-05-D-5610 (Task Order 0004, Project 4-011) and FA8650-11-D-5610 (Task Order 0001, Project 1-040 and Task Order 0006, Project 6-002) by UDRI under direction of AFRL's Materials Integrity Branch (AFRL/RXSA). Kara Storage (AFRL/RXSA) served as the contract monitor. The following provided technical advice throughout the project: Ryan Osysko, Kevin Davis, Al Fletcher and Chad Hunter of AFRL's Systems Support Division (AFRL/RXS); Rodney Coulter (WR-ALC/MXDEC); Ken Patterson (AFLCMC/EZPT-ACO); Jason Cary, Dave Nielson and Brandon Smith (AFLCMC/WWUV); Jacob Shults and Brandon Malloy (Air Force maintainers); Bryan Adkins (Marine maintainer); Daniel Pritchett (Navy maintainer); Steve Twaddle and Eric Atkins (Lockheed Martin); and Paul Barnum, Karl Batig, Rob Berg, Wayne Cox, Mike Fleischmann, Ken Hollingsworth, Sara McIntosh, Don Mottor, Jake Parks, Pete Sciandra, Paul Smith and Beau Turner (Northrop Grumman Corporation). Brad Pinnell (UDRI) performed the photomicroscopy. Technical advice and material support were provided by Bruce Hackett (AFC Tools); Tom Mendel, Anthony Malone and Heidi Page (Performance Plastics, LTD); and Lynn Robinson (Noble Tools). Development support was also provided by Lucas Abrahamson and Christian Pfledderer (Southwestern Ohio Council for Higher Education). Legal advice and patent support were provided by Candise Powell and Mathew Willenbrink (the University of Dayton Technology Partnership Office). This paper was cleared per case number 88ABW-2018-0867.

7. REFERENCES

1. Childers, P.K. and Osysko, R.P., “Nonmetallic Rotary Gap Filler Removal Bit,” Composites Manufacturing Conference, Mesa, AZ, 13-15 March 2012.
2. Osysko, R.P. and Childers, P.K., “Development and Evaluation of Nonmetallic Rotary Gap Filler Removal Bits,” STAR #13-001 (report), 7 February 2013.
3. Mazza, J.J. and Childers, P.K., “Reduced Structural Damage Using New Nonmetallic Material Removal Tools,” Aircraft Airworthiness & Sustainment Conference, Phoenix, AZ, 22-25 May 2017.